© 2016. Published by The Company of Biologists Ltd | Development (2016) 143, 516-529 doi:10.1242/dev.129957

RESEARCH ARTICLE

Differentiation and molecular heterogeneity of inhibitory and excitatory neurons associated with midbrain dopaminergic nuclei

Laura Lahti[1], Maarja Haugas[1], Laura Tikker[1], Mikko Airavaara[2], Merja H. Voutilainen[2], Jenni Anttila[2], Suman Kumar[1], Caisa Inkinen[1], Marjo Salminen[3] and Juha Partanen[1,*]

ABSTRACT

Local inhibitory GABAergic and excitatory glutamatergic neurons are important for midbrain dopaminergic and hindbrain serotonergic pathways controlling motivation, mood, and voluntary movements. Such neurons reside both within the dopaminergic nuclei, and in adjacent brain structures, including the rostromedial and laterodorsal tegmental nuclei. Compared with the monoaminergic neurons, the development, heterogeneity, and molecular characteristics of these regulatory neurons are poorly understood. We show here that different GABAergic and glutamatergic subgroups associated with the monoaminergic nuclei express specific transcription factors. These neurons share common origins in the ventrolateral rhombomere 1, where the postmitotic selector genes *Tal1*, *Gata2* and *Gata3* control the balance between the generation of inhibitory and excitatory neurons. In the absence of Tal1, or both Gata2 and Gata3, the GABAergic precursors adopt glutamatergic fates and populate the glutamatergic nuclei in excessive numbers. Together, our results uncover developmental regulatory mechanisms, molecular characteristics, and heterogeneity of central regulators of monoaminergic circuits.

KEY WORDS: Neurogenesis, Tal1, Gata2, Gata3, Transcription factor, VTA, SNpr, RMTg, GABA, Glutamate, Dopamine, Serotonin, Midbrain, Hindbrain, Mouse, Chicken

INTRODUCTION

Midbrain dopaminergic (DA) and dorsal raphe serotonergic (5-HT) neurons regulate responses to reward and punishment, associative learning, mood, and coordination of voluntary movements. Function of these monoaminergic pathways is controlled by inhibitory and excitatory neurons, including important populations residing locally within the monoaminergic nuclei as well as in the adjacent midbrain and anterior hindbrain (Russo and Nestler, 2013; Lammel et al., 2014; Proulx et al., 2014; Morello and Partanen, 2015). Dysfunction of monoaminergic circuits is thought to lead to a multitude of psychiatric and neurophysiological disorders, such as schizophrenia, depression, addiction and Parkinson's disease. Understanding these complex disorders requires knowledge of the various components of these networks. However, compared with monoaminergic neurons themselves, very little is known about the development and heterogeneity of their regulators.

[1]Department of Biosciences, P.O. Box 56, Viikinkaari 9, FIN-00014 University of Helsinki, Helsinki, Finland. [2]Institute of Biotechnology, P.O. Box 56, Viikinkaari 9, FIN-00014 University of Helsinki, Helsinki, Finland. [3]Department of Veterinary Biosciences, P.O. Box 66, Agnes Sjöbergin katu 2, FIN-00014 University of Helsinki, Helsinki, Finland.

*Author for correspondence (juha.m.partanen@helsinki.fi)

Received 18 August 2015; Accepted 18 December 2015

Inhibitory signals to DA neurons, located in the ventral tegmental area (VTA), substantia nigra pars compacta (SNpc) and retrorubral field (RRF), arrive from neighbouring GABAergic neurons in the VTA, substantia nigra pars reticulata (SNpr) and rostromedial tegmental nucleus (RMTg, also called the tail of VTA) (Perrotti et al., 2005; Jhou et al., 2009a,b; Kaufling et al., 2009; Zhou and Lee, 2011; Cohen et al., 2012; Lammel et al., 2012; Margolis et al., 2012; Yetnikoff et al., 2015). Collectively, these GABAergic neurons are referred to as dopaminergic neuron-associated GABAergic (D-GABA) neurons (Lahti et al., 2013). It has been suggested that the RMTg integrates signals from different parts of the brain, including the lateral habenula (LHb), converting them into inhibitory inputs to both DA and 5-HT networks (Lavezzi and Zahm, 2011; Barrot et al., 2012; Bourdy and Barrot, 2012; Proulx et al., 2014; Sego et al., 2014).

Excitatory glutamatergic inputs to DA neurons come from a number of brain regions, including the laterodorsal tegmental nucleus (LDTg) in the anterior hindbrain (Geisler et al., 2007; Lammel et al., 2012). Recent studies have also identified glutamatergic neurons embedded in the DA nuclei themselves and these may provide local excitatory neurotransmission (Morales and Root, 2014). Moreover, the interpeduncular nucleus (IPN) below the DA and RMTg nuclei can relay excitatory input to monoaminergic neurons, in particular the 5-HT system (Groenewegen et al., 1986; Proulx et al., 2014; Antolin-Fontes et al., 2015).

The GABAergic and glutamatergic neurons within the DA nuclei also have targets other than the DA neurons. GABAergic SNpr is the main output source of the basal ganglia and projects to brain regions important for activation of voluntary movements. Furthermore, some VTA GABAergic and glutamatergic neurons project to the forebrain and regulate pathways involved in associative learning (Fields et al., 2007; Brown et al., 2012; Kabanova et al., 2015).

Our previous work has shown that the majority of D-GABA neurons are born outside the midbrain in the anterior rhombomere 1 (r1) (Achim et al., 2012). The r1 generates multiple neuronal subtypes in different dorsoventral domains characterized by specific combinations of transcription factors (Waite et al., 2012; Lahti et al., 2013). Expression of *Nkx6-1* in the ventricular zone and *Gata2* and *Tal1* (also known as *Scl*) in the corresponding mantle zone was suggested to specify the ventrolateral r1 domain contributing to D-GABA neurons (Achim et al., 2012). Because of molecular similarity to the spinal cord V2 domain, we call this region rhombencephalic V2 (rV2) (previously referred to as the GABA I domain; Lahti et al., 2013). Of the rV2 factors, Gata2 is dispensable for development of D-GABA neurons, whereas inactivation of *Tal1* leads to a specific loss of the majority of GABAergic neurons in the SNpr (Kala et al., 2009; Achim et al., 2012, 2013). However, these studies left open the exact role of Tal1 as well as its co-factors and downstream effectors during neuronal differentiation in rV2.

Development (2016) 143, 516-529 doi:10.1242/dev.129957

Here, we characterized the diversity of neurons generated in the ventral r1. We show that, in addition to GABAergic neurons of the SNpr, VTA and RMTg, the rV2 domain gives rise to glutamatergic neurons in the SNpc, VTA, IPN and LDTg. Thus, our findings reveal that these neurons, all components of the DA and 5-HT regulatory circuits, share a common developmental history. Importantly, the balance between rV2 inhibitory and excitatory neurons is controlled by Tal1, which cooperates with both Gata2 and Gata3. Although these factors are activated independently of each other, together they promote GABAergic and suppress glutamatergic identity as postmitotic selector genes. Furthermore, we discovered a set of transcription factors, which are activated downstream of Gata/Tal selectors, and are expressed differentially in D-GABA neuron subgroups, providing novel molecular markers for them and exposing heterogeneity within and between these nuclei.

RESULTS

GABAergic subtypes generated in ventral r1

Embryonic r1 generates several different subsets of GABAergic neuron precursors expressing specific combinations of transcription factors. Diversity and contribution of these precursors to brain nuclei are poorly understood. We aimed to characterize the GABAergic subtypes generated in the ventral r1, focusing on the identification of D-GABAergic precursors. As we had previously shown that the peak of D-GABA precursor generation is at

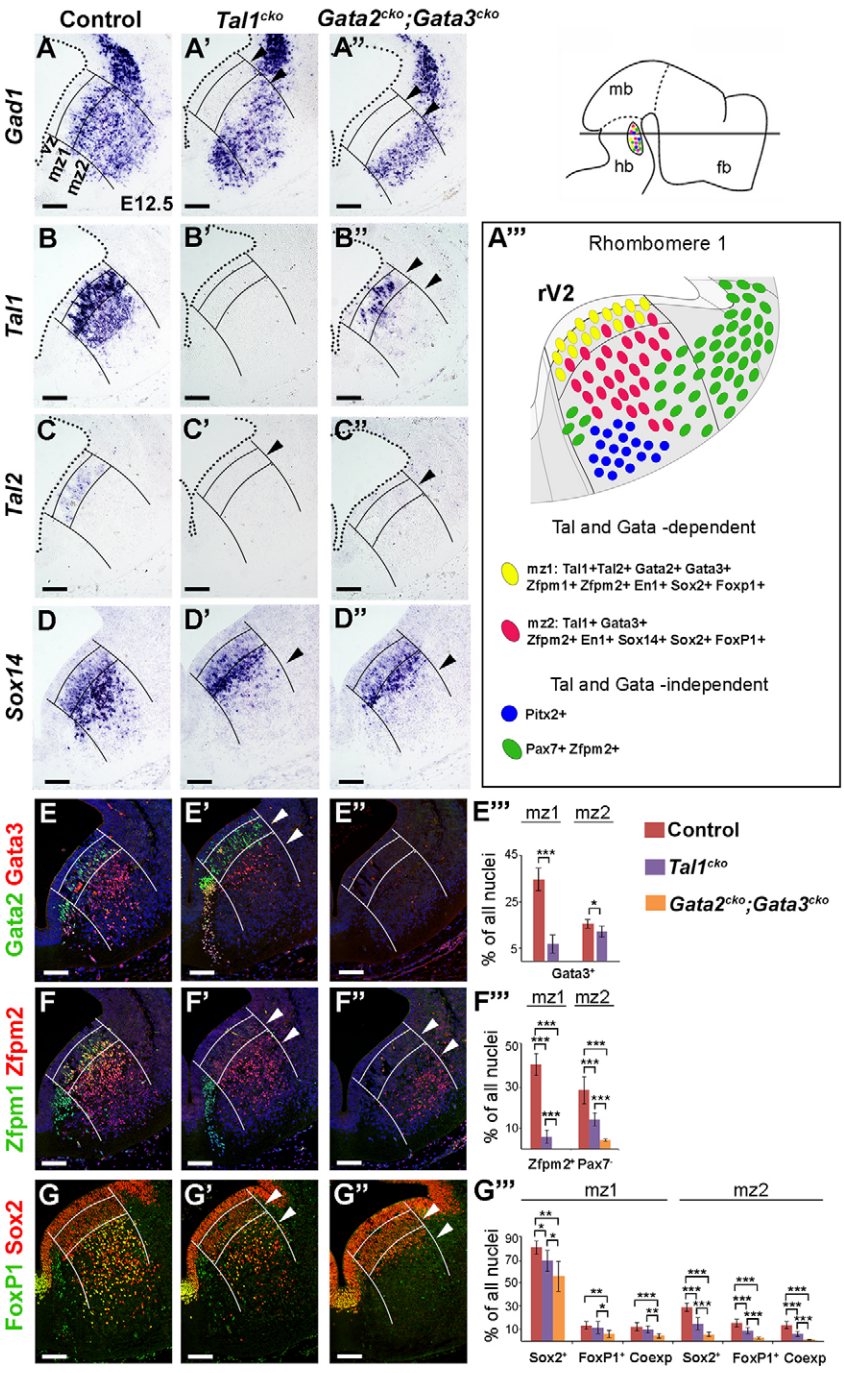

Fig. 1. Subtypes of GABAergic precursors in r1 and their dependency on Tal1, Gata2 and Gata3. (A-G″) ISH (A-D″) and IHC (E-G″) on E12.5 control, *Tal1*^{cko} and *Gata2*^{cko};*Gata3*^{cko} r1. The level of sectioning is shown in the diagram (top right). The ventricular surface is indicated with a dotted line (A-C″). The rV2 domain is indicated with a line and divided into ventricular zone (vz), mantle zone 1 (mz1) and mantle zone 2 (mz2). Arrowheads point to altered expression. (A‴) Model of E12.5 ventral r1 depicting the heterogeneity of the main GABAergic subtypes and their dependency on Tal1, Gata2 and Gata3. (E‴-G‴) The percentage of Gata3$^+$ (E‴), Zfpm2$^+$Pax7$^-$ (F‴), Sox2$^+$, FoxP1$^+$ and Sox2$^+$FoxP1$^+$ (Coexp) (G‴) nuclei in mz1 and mz2 of control and mutant embryos (average with s.d.). *P<0.05, **P<0.01, ***P<0.001. fb, forebrain; hb, hindbrain; mb, midbrain. Scale bars: 200 µm.

Development (2016) 143, 516-529 doi:10.1242/dev.129957

embryonic day (E) 11.5-12.5 (Achim et al., 2012), after which time they start to migrate towards the midbrain, we chose the E12.5 stage for the analysis.

As shown previously (Achim et al., 2012), a subset of postmitotic GABAergic precursors in the ventrolateral rV2 domain expressed *Tal1* (Fig. 1A,B). In addition, the same region expressed the functionally related factors *Tal2*, *Gata2* and *Gata3* (Fig. 1C,E). In our separate experiments, gene expression profiling of *Gata2* mutant midbrain revealed putative Gata/Tal factor targets, including Gata co-factors *Zfpm1* and *Zfpm2* (also known as *Fog1* and *Fog2*, respectively) as well as the transcription factors *FoxP1*, *Sox14* and *Six3* (K. Achim, L.L., M.S. and J.P., unpublished). Of these, *Sox14*, *Zfpm1*, *Zfpm2* and *FoxP1* were also expressed in the rV2 domain (Fig. 1D,F,G). In addition, the rV2 domain expressed Sox2 and *En1* (Fig. 1G, Fig. S1B,G). These 11 transcription factors were co-expressed also at the cellular level (Fig. 1E-G; Fig. S1F-M). However, their patterns were complex and divided the GABAergic precursors in the rV2 domain into subgroups. More specifically, the mantle zone (mz) could be divided apicobasally into two domains: the more apical mz1 expressed all the factors, whereas more basal mz2 lacked *Gata2*, *Tal2* and *Zfpm1*. As *Gata2*, *Tal2* and *Zfpm1* are mostly not detected in the midbrain and hindbrain neurons later in embryogenesis (Kala et al., 2009; Achim et al., 2013) (data not shown), their expression patterns might reflect dynamic gene expression changes during neuronal maturation, suggesting that postmitotic precursors in mz1 are only beginning their differentiation process. Moreover, the GABAergic precursors within mz1 and mz2 were heterogeneous. For example, in mz1, Zfpm2 colocalized with Zfpm1 and Gata3, and in mz2 with Gata3 or En1 in a subset of cells (Fig. 1F; Fig. S1F-Ka). In mz2, approximately half of the $Sox2^{+}$ cells co-expressed FoxP1 (Fig. 1G,G‴). Furthermore, the majority of these $Sox2^{+}FoxP1^{+}$ cells expressed the transcription factor *Sox14* (Fig. S1L-Ma).

In addition, subsets of GABAergic precursors in the ventral r1 express *Pitx2* and *Pax7* (Aroca et al., 2006; Waite et al., 2012). $Pax7^{+}$ precursors appeared to originate from the more dorsal r1, where the ventricular zone progenitors also expressed Pax7 (Fig. S1E-Eb). This is also supported by gene expression and fate-mapping data from avian embryos (Lorente-Canovas et al., 2012). We found that some $Pax7^{+}$ precursors co-expressed Zfpm2 but no other Gata- or Tal-related factors (Fig. S1E; data not shown). Thus, the $Zfpm2^{+}$ cells in the rV2 domain can be divided into $Zfpm2^{+}Pax7^{+}$ and $Zfpm2^{+}Pax7^{-}$ subgroups (see above). $Pitx2^{+}$ cells were located in the most basal part of mz2 throughout the entire r1, and did not express Gata or Tal factors or their putative targets (Fig. S1C; data not shown).

GABAergic neuron subtypes dependent on Tal and Gata factors in r1

We previously showed that conditional knockout (cko) of *Tal1* in the mouse leads to a loss of GABAergic neurons in the SNpr (Achim et al., 2012). In order to elucidate which of the r1 GABAergic precursor subgroups contributed to this loss of D-GABA nuclei in $Tal1^{cko}$ mutants, we aimed to identify Tal1-dependent precursors. Consistent with our earlier report (Achim et al., 2012), *Gad1* expression in the rV2 domain of $Tal1^{cko}$ mice was downregulated in mz1 and partly also in mz2 (Fig. 1A′). In mz2, the remaining GABAergic cells represented mostly $Pitx2^{+}$ and $Pax7^{+}$ subtypes, which appeared to be unaffected in mutants (Fig. S1C′,E′). In $Tal1^{cko}$ mz1, *Tal2* and *Zfpm1* were downregulated completely (Fig. 1C′,F′). Although we found that *Gata2* and *Gata3* were activated independently of *Tal1*, in $Tal1^{cko}$ mice the number of $Gata3^{+}$ cells was nevertheless significantly lower (Fig. 1E′,E‴). In addition, a significant fraction of $Zfpm2^{+}Pax7^{-}$, $Sox2^{+}$, $FoxP1^{+}$ and $Sox2^{+}FoxP1^{+}$ cells was absent in mutants, indicating that these subtypes are largely Tal1 dependent (Fig. 1F′,F‴,G′,G‴). *Sox14* was still expressed in $Tal1^{cko}$ mice, although the number of *Sox14*-positive cells appeared to be lower in the lateral mz2 (Fig. 1D′).

In the haematopoietic system, Tal1 works in a complex with the Gata factors Gata1 and Gata2 (Wadman et al., 1997). As *Gata2* and *Gata3* are also expressed in the rV2 domain, we investigated whether they could cooperate with Tal1 and whether the residual GABAergic cells in $Tal1^{cko}$ r1 could be *Gata2* or *Gata3* dependent. In single $Gata2^{cko}$ and $Gata3^{cko}$ mutants, all GABAergic markers appeared to be unaffected (Fig. S2). This supports our earlier observations of intact D-GABA neurons in E18.5 $Gata2^{cko}$ and $Gata3^{cko}$ midbrain (Kala et al., 2009; Achim et al., 2012, 2013). By contrast, when both genes were inactivated together ($Gata2^{cko}$; $Gata3^{cko}$) the phenotype resembled that of the $Tal1^{cko}$ mutant (Fig. 1A″-G‴; Fig. S1B″-E″). Although *Tal1* itself was activated

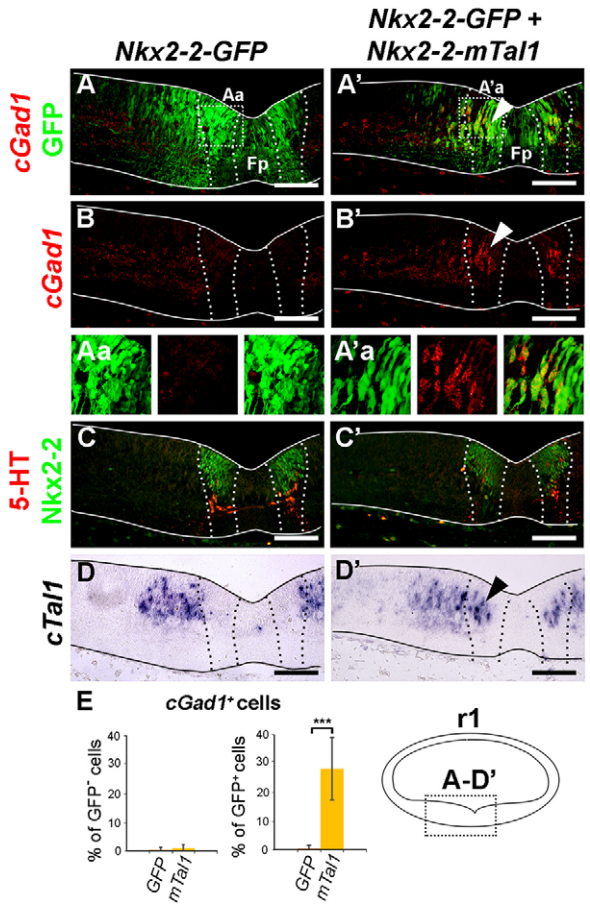

Fig. 2. Induction of GABAergic differentiation by *Tal1* overexpression in chicken serotonergic domain. (A-D′) IHC combined with ISH (A-B′), IHC (C,C′) and ISH (D,D′) on transverse adjacent sections of HH26-29 chicken r1. Solid lines delineate the r1 tissue, dotted lines the 5-HT domain. Embryos were electroporated with *Nkx2-2-GFP* (A-D), or both *Nkx2-2-GFP* and *Nkx2-2-mTal1* (A′-D′) plasmids. Arrowheads point to altered expression. Aa and A′a show higher magnification single-channel and merged images of the indicated areas of A and A′, respectively. The region shown in A-D′ is indicated in the diagram (bottom right). (E) Quantification of $cGad1^{+}$ cells among the GFP^{+} and GFP^{-} cells in the serotonergic domain of control (GFP) and mTal1-overexpressing embryos (n=4; averages with s.d.). 5-HT, 5-hydroxytryptophan; Fp, floor plate. Scale bars: 100 µm.

Development (2016) 143, 516-529 doi:10.1242/dev.129957

independently of Gata2 and Gata3, the maintenance of its expression appeared to fail, as *Tal1* expression was downregulated in the mz2 region of the *Gata2*^{cko};*Gata3*^{cko} mutants (Fig. 1B″). Compared with *Tal1*^{cko} r1, the number of Zfpm2^{+}, Sox2^{+} and FoxP1^{+} cells in *Gata2*^{cko};*Gata3*^{cko} r1 was reduced even further (Fig. 1F′-G‴). Again, Pitx2^{+} and Pax7^{+} cells remained unaffected, demonstrating that these subtypes represent GABAergic precursors that are independent of *Tal1*, *Gata2* and *Gata3* regulation (Fig. S1C″,E″).

Taken together, our results demonstrate that the embryonic rV2 domain contains a variety of GABAergic precursors (Fig. 1A‴), a large fraction of which redundantly require Gata2 or Gata3. Most, but not all, of these Gata2/3-dependent precursors are also Tal1 dependent and consist of Tal2^{+}, Gata3^{+}, Zfpm1^{+}, Zfpm2^{+}, En1^{+}, Sox2^{+}, FoxP1^{+} and Sox14^{+} cells, which express these transcription factors in different combinations. In addition, the Gata2/3-independent GABAergic neurons in the lateral mz2, mostly Pitx2^{+}or Pax7^{+}, appear to represent developmentally distinct subgroups of r1 GABAergic neurons.

Tal1 can modulate the function of Gata factors

Given the similarity of *Gata2*^{cko};*Gata3*^{cko} and *Tal1*^{cko} mutants, we investigated whether Tal1 can affect the function of Gata factors. In addition to GABAergic precursors, *Gata2* and *Gata3* are expressed in 5-HT precursors located ventrally to the rV2 region and are needed for the 5-HT phenotype (Craven et al., 2004; Pattyn et al., 2004; Kala et al., 2009) (our unpublished results). We speculated that the neuronal subtype identities regulated by Gata factors – GABAergic or 5-HT, depending on the region – could be influenced by *Tal1*, which is largely absent from 5-HT precursors. Thus, introducing Tal1 in the Gata2/3 complex might turn on a different set of downstream genes.

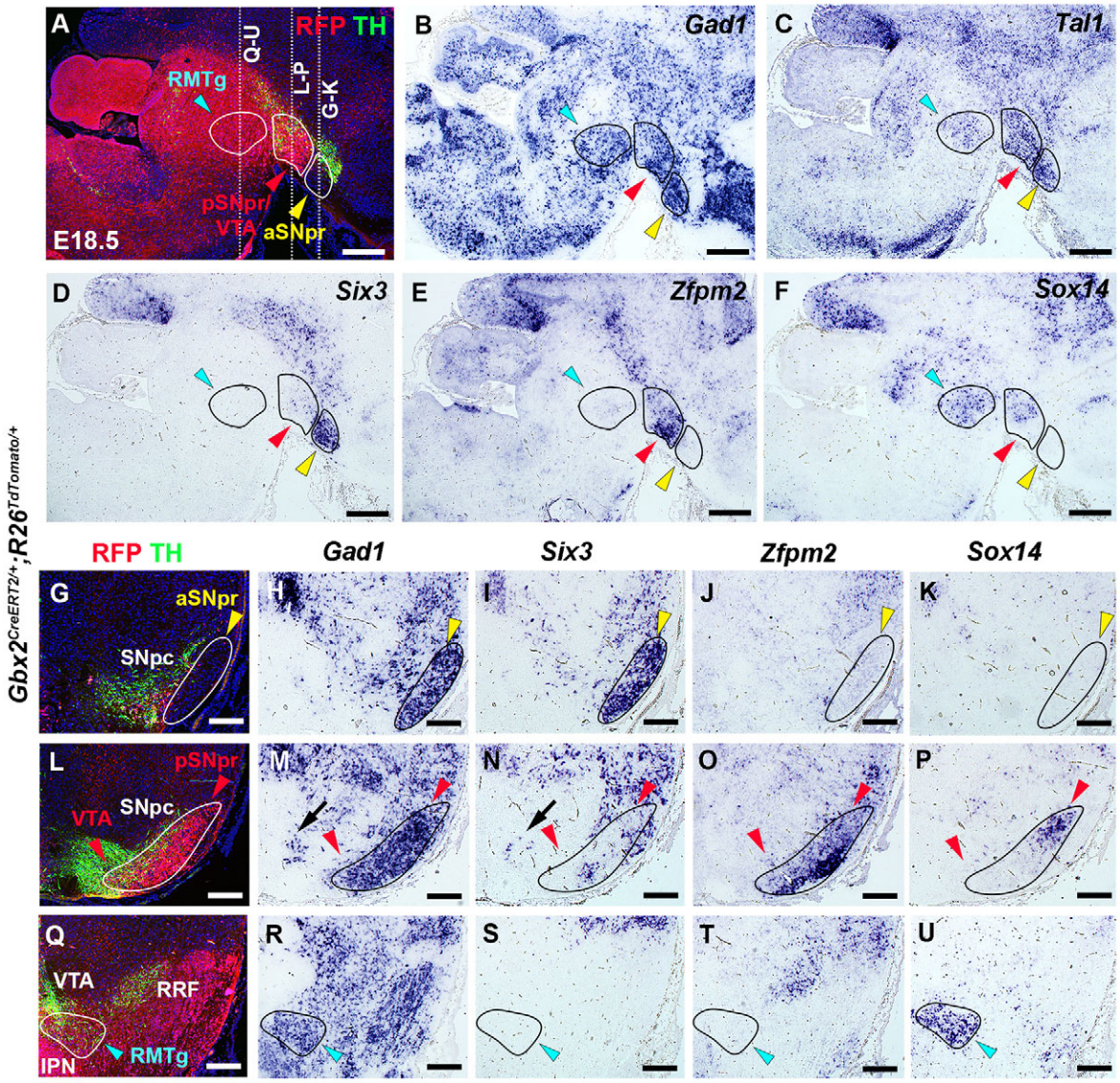

Fig. 3. Expression of *Sox14*, *Zfpm2* and *Six3* in distinct D-GABAergic nuclei. (A-F) IHC (A) and ISH (B-F) on adjacent sagittal sections of an E18.5 *Gbx2*^{CreERT2};*R26*^{TdTomato} embryo. D-GABAergic nuclei are encircled. (G-U) IHC (G,L,Q) and ISH (H-K,M-P,R-U) on coronal sections of similar embryos, sectioning planes as indicated in A. Arrows point to the parabrachial pigmented subnucleus of the VTA (M,N). Coloured arrowheads point to the anatomical regions indicated in A,G,L,Q. aSNpr, anterior substantia nigra pars reticulata; IPN, interpeduncular nucleus; pSNpr, posterior substantia nigra pars reticulata; RMTg, rostromedial tegmental nucleus; RRF, retrorubral field; SNpc, substantia nigra pars compacta; VTA, ventral tegmental area. Scale bars: 400 µm (A-F); 200 µm (G-U).

Development (2016) 143, 516-529 doi:10.1242/dev.129957

To investigate this, we electroporated Hamburger–Hamilton stage (HH) 14-16 chicken ventral r1 with an *Nkx2-2-mTal1* construct. This vector drives expression of mouse *Tal1* under the *Nkx2-2* enhancer in the serotonergic domain. Indeed, 48 h after the electroporation, mouse *Tal1* overexpression resulted in the appearance of chicken *Gad1* and *Tal1* transcripts and reduction of the 5-HT markers 5-hydroxytryptophan and *cLmx1b* in the Nkx2-2 domain (Fig. 2A-D′; data not shown). Expression of *cGad1* was induced specifically in cells electroporated with the *Nkx2-2-mTal1* vector (Fig. 2E). Taken together, the results from gain-of-function experiments and conditional mutagenesis suggest that the presence of Tal1, Gata2 and Gata3 together is both necessary and sufficient to induce GABAergic identity in ventral r1.

We then investigated whether loss of *Tal1* from rV2 would redirect GABAergic precursors into a 5-HT phenotype. No ectopic expression of 5-HT markers was detected in the $Tal1^{cko}$ mice (Fig. S1N,N′). Instead, the precursors are redirected to an alternative rV2 region-specific phenotype (see below).

Distinct transcription factors downstream of Gata/Tal selectors mark different D-GABA neuron subgroups

After discovering *Tal1* and *Gata2/3* -dependent GABAergic precursor subtypes and their markers in the embryonic r1, we investigated whether we could detect them later within hindbrain-derived D-GABAergic nuclei. For this, we utilized $Gbx2^{CreERT2}$;$R26^{TdTomato}$ embryos, in which r1-derived tissue expressed red fluorescent protein (RFP) allowing us to follow migration of D-GABAergic precursors to ventral midbrain (Fig. 3A,G,L,Q; Fig. S3). At E18.5, all *Gad1*-expressing D-GABA nuclei expressed *Tal1* (Fig. 3A-C), but showed differences in *Sox14*, *Zfpm2* and *Six3* expression. The RFP-negative anterior SNpr (aSNpr), identifiable by *Six3* expression (Madrigal et al., 2015), lacked *Zfpm2* and *Sox14* expression (Fig. 3D-K). Indeed, in the rV2-domain at E12.5 *Six3* was not detected (Fig. S1D-D″), consistent with a different origin of aSNpr. By contrast, the RFP-labelled and *Six3*-negative posterior SNpr (pSNpr) expressed *Sox14* in its laterodorsal region and *Zfpm2* throughout (Fig. 3D-F,L-P). The few *Six3*-expressing cells among $Zfpm2^{+}$ cells in pSNpr were RFP negative and not found in the more posterior regions (Fig. 3N; data not shown). In the VTA, the lateral regions contained few $Zfpm2^{+}$ cells detectable by immunohistochemistry (IHC) but not by *in situ* hybridization (ISH) (Fig. 3O; Fig. S4B). However, the parabrachial pigmented nucleus (PBP) of the medial VTA contained few *Six3*-expressing GABAergic cells, which were also RFP negative (Fig. 3L-N). Posteriorly, the RFP-labelled RMTg lacked both *Zfpm2* and *Six3* transcripts but expressed *Sox14* strongly (Fig. 3D-F,Q-U).

Thus, these data indicate that *Six3*, *Zfpm2* and *Sox14* expression characterize different D-GABA nuclei, with *Zfpm2*-expressing neurons contributing mostly to pSNpr and *Sox14*-expressing neurons to RMTg. The *Six3* transcripts were found in the anterior SNpr and PBP, which appear to comprise developmentally and molecularly distinct subnuclei.

Development and molecular heterogeneity of GABAergic neurons in pSNpr and VTA

As a subset of $Zfpm2^{+}$ cells in the E12.5 r1 co-expressed Gata3 and En1, we investigated whether these subtypes could be found in the pSNpr. Indeed, at E18.5 this nucleus contained $Zfpm2^{+}$ cells, some of which co-expressed Gata3 and En1 (Fig. S4A-Fa). The most

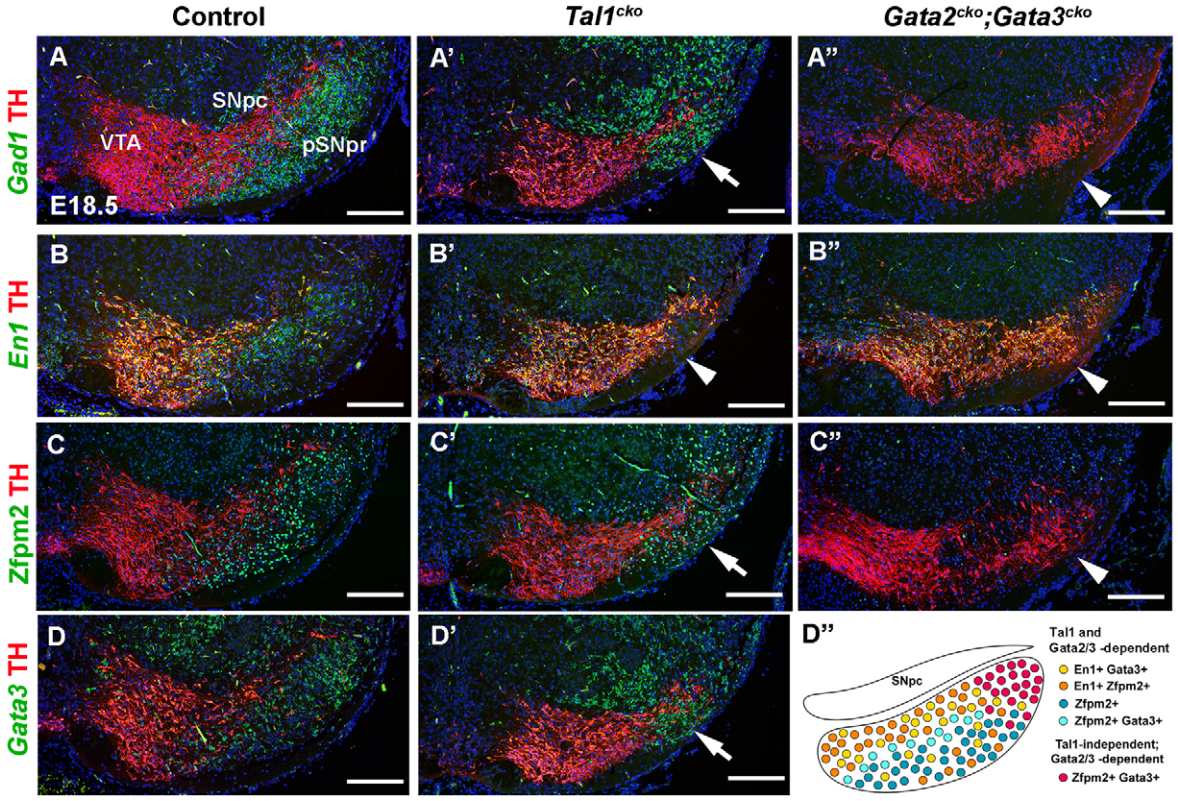

Fig. 4. pSNpr and VTA GABAergic neuron markers in $Tal1^{cko}$ and $Gata2^{cko}$;$Gata3^{cko}$ mutants. (A-D′) Fluorescent ISH and IHC (A-B″,D,D′) and IHC (C-C″) on adjacent coronal sections of E18.5 control, $Tal1^{cko}$ and $Gata2^{cko}$;$Gata3^{cko}$ midbrain. Arrowheads point to loss of expression. Arrows point to remaining *Gad1*-, *Zfpm2*- and *Gata3*-expressing cells. (D″) Model of GABAergic subtypes in the pSNpr at E18.5. SNpc, substantia nigra pars compacta; pSNpr, posterior substantia nigra pars reticulata; VTA, ventral tegmental area. Scale bars: 200 µm.

Development (2016) 143, 516-529 doi:10.1242/dev.129957

basal pSNpr consisted of a group of Zfpm2^{+} cells, which largely lacked both Gata3 and En1. In turn, pSNpr contained also Gata3^{+} and En1^{+} cells lacking Zfpm2, as well as Gata3^{+} cells expressing *En1* transcripts (Fig. S4Ca,Fa,G-Ia). In the adult pSNpr, the expression of these factors was still detectable (data not shown).

Next, we investigated whether the difference between the amount of Zfpm2^{+} and Gata3^{+} cells in E12.5 *Tal1*^{cko} and *Gata2*^{cko};*Gata3*^{cko} r1 was reflected in pSNpr at E18.5 (Fig. 4). Indeed, similar to the E12.5 r1, *Tal1*^{cko} mutant pSNpr still contained some Zfpm2^{+} and Gata3^{+} GABAergic cells in the most lateral domain, whereas in *Gata2*^{cko};*Gata3*^{cko} mutants the Zfpm2^{+} cells were completely absent (Fig. 4A-A″,C-C″,D,D′). By contrast, again correlating with the E12.5 phenotype, both mutants lacked all GABAergic neurons expressing *En1* (Fig. 4B-B″). In *Gata2*^{cko} and *Gata3*^{cko} single mutants, the expression of these markers in pSNpr appeared to be unaffected (data not shown).

Taken together, the pSNpr contains both Tal1-dependent neurons expressing combinations of *En1*, *Gata3* and *Zfpm2*, as well as Tal1-independent subtypes expressing *Zfpm2* and *Gata3*. All of these appear to be Gata2/3 dependent (Fig. 4D″).

Molecular markers and development of RMTg GABAergic neurons

As we had detected *Sox14*, *Sox2* and *FoxP1* co-expressing cells in E12.5 r1, we investigated whether *Sox14*$^{+}$ RMTg neurons expressed all these factors. Indeed, all *Sox14*, FoxP1 and Sox2 were present in the same RMTg cells at E18.5 (Fig. 5A-I), and appeared to be specific to this subgroup of GABAergic neurons (Fig. 5M-Oa; data

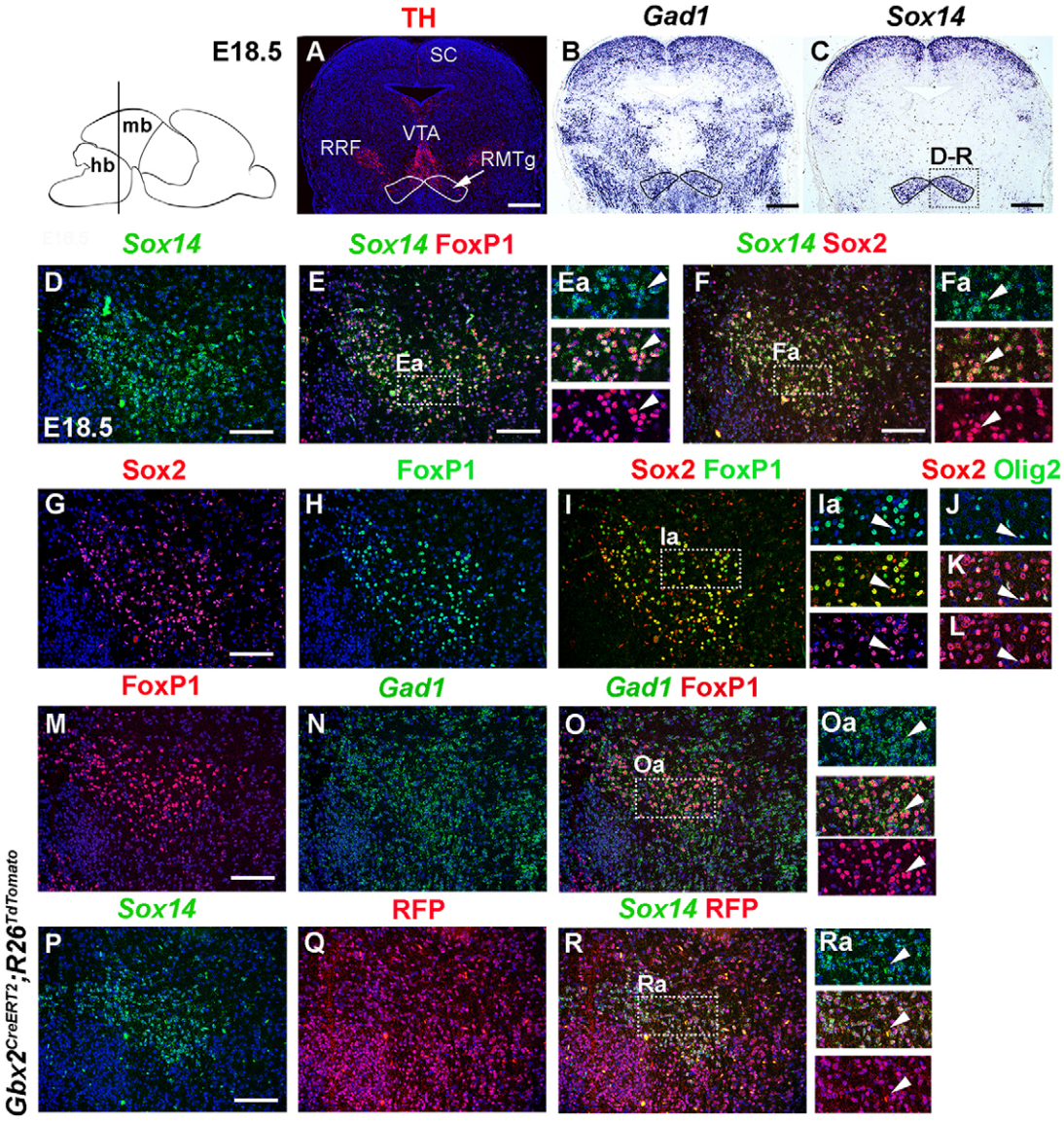

Fig. 5. Expression of *Sox14*, Sox2 and FoxP1 in the embryonic RMTg. (A-C) IHC (A) and ISH (B,C) on adjacent coronal sections of E18.5 brain. Boxed area in C indicates the region shown in D-R. (D-F) *Sox14* fluorescent ISH with FoxP1 (E) and Sox2 (F) IHC. (G-I) Sox2 and FoxP1 IHC. (J-L) Sox2 and Olig2 IHC on a section parallel to that shown in I, from the same area as Ia. (M-O) FoxP1 IHC with *Gad1* ISH. (P-R) *Sox14* fluorescent ISH and RFP IHC on a *Gbx2*^{CreERT2};*R26*^{TdTomato} brain. Ea, Fa, Ia, Oa and Ra show higher magnification single-channel and merged images of the indicated areas of E, F, I, O and R, respectively. Arrowheads point to co-expressing cells. hb, hindbrain; mb, midbrain; RMTg, rostromedial tegmental nucleus; RRF, retrorubral field; SC, superior colliculus; VTA, ventral tegmental area. Scale bars: 200 µm.

Development (2016) 143, 516-529 doi:10.1242/dev.129957

not shown). The *Sox14*- and FoxP1-negative Sox2^{+} cells turned out to be Olig2^{+} (Fig. 5J-L), indicating a glial identity (Hoffmann et al., 2014). Furthermore, the expression of *Sox14*, FoxP1 and Sox2 colocalized with Gbx2^{CreERT2}-labelled RFP^{+} cells supporting the origin of RMTg in the r1 (Fig. 5P-Ra).

In the adult brain, FoxP1^{+} cells were found between the caudal VTA and IPN, in the area corresponding to the *Sox14*$^{+}$Sox2^{+}FoxP1^{+} nucleus in perinatal embryos, but they lacked both *Sox14* transcripts and Sox2 (data not shown). We wanted to confirm that these FoxP1^{+} cells corresponded to the RMTg. This nucleus can be currently identified by two main methods: retro- or anterograde labelling from the VTA/SNpc or LHb, respectively, or methamphetamine-induced expression of the protein encoded by the immediate early gene FosB (Perrotti et al., 2005; Jhou et al., 2009a,b; Kaufling et al., 2009). For anterograde labelling of the RMTg, we injected mice with AAV2-GFP into the LHb (Fig. 6A). In these mice, GFP-positive projections descending from the LHb made highly specific contacts with the GABAergic FoxP1^{+} nucleus (Fig. 6B,C). Next, we administered methamphetamine to wild-type mice and compared the expression of FosB and FoxP1 in the RMTg. Whereas in NaCl-treated control animals the FoxP1^{+} cells were negative for FosB, in metamphetamine-treated animals we detected co-expression of FoxP1 and FosB in numerous cells in this region (Fig. 6D-K). These results together indicate that the FoxP1^{+} neuronal population corresponds to the RMTg.

As FoxP1, Sox2 and *Sox14* transcripts were downregulated in the *Tal1*^{cko} and *Gata2*^{cko};*Gata3*^{cko} r1 at E12.5, we wanted to investigate whether the RMTg was affected in these mutants. Indeed, in the area corresponding to the RMTg in wild-type embryos, no *Gad1*-expressing nucleus containing Sox2, FoxP1 or *Sox14*-expressing cells was found in mutants (Fig. 7). The RMTg of *Gata2*^{cko} and *Gata3*^{cko} single mutants appeared normal (Fig. S5).

In summary, our results suggest that development of the RMTg requires Tal and Gata factors. Moreover, *Sox14*, Sox2 and FoxP1 can be used as molecular markers for the RMTg during embryogenesis, and FoxP1 also in the adult brain.

Development and molecular diversity of glutamatergic neurons in IPN, LDTg and SNpr

The transcription factor profile of rV2 domain resembles the spinal cord p2/V2 domain, which generates not only GABAergic, but also Vsx2^{+} (also known as Chx10) glutamatergic neurons from Nkx6-1^{+} progenitors (Arber, 2012). To elucidate whether the rV2 domain produces glutamatergic neurons, we analysed Nkx6-1 and Vsx2 expression at E12.5. As reported previously (Waite et al., 2012), Nkx6-1 was detected in all rV2 progenitors, and in a subset of postmitotic precursors (Fig. 8A,C′). The majority of these Nkx6-1^{+} precursors co-expressed Vsx2 (Fig. 8B-C′). During development, these precursors started to separate into Nkx6-1^{+}, Vsx2^{+}, and Nkx6-1^{+}Vsx2^{+} subpopulations, upregulated a glutamatergic marker *Slc17a6* (also known as *Vglut2*), and some of them migrated anteriorly towards the midbrain (Fig. S6A-I; data not shown). In E16.5 and E18.5 midbrain, we found these three different subtypes

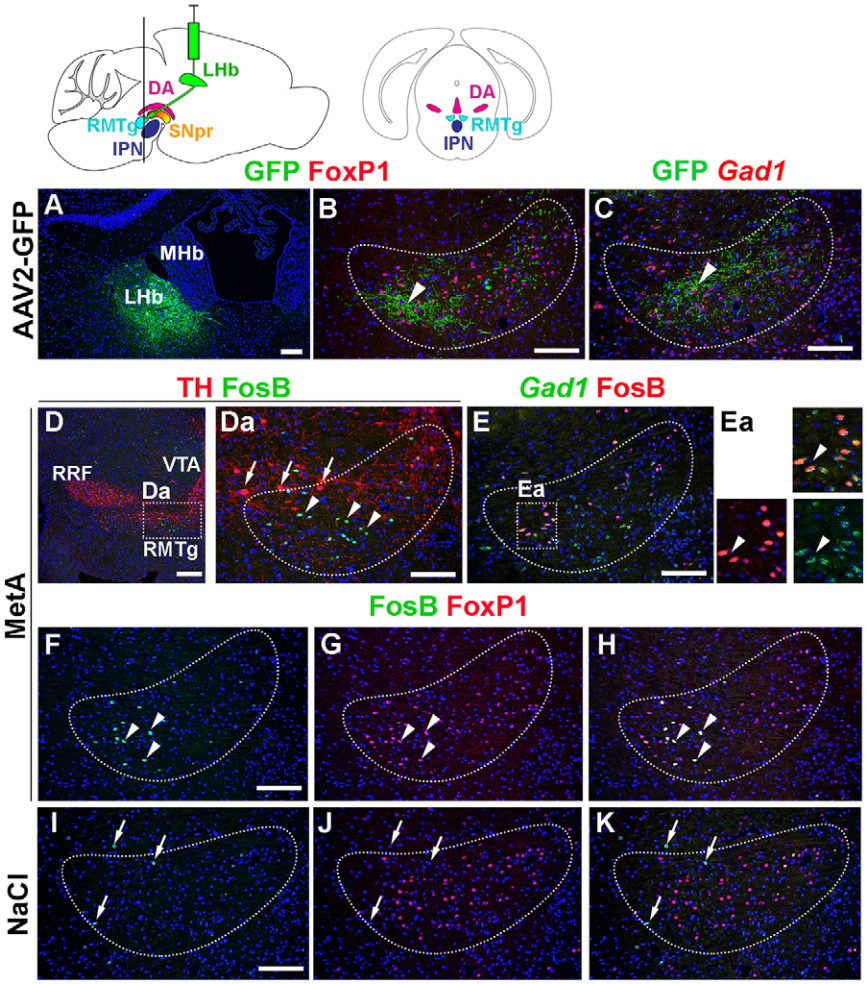

Fig. 6. Expression of FoxP1 in the adult RMTg. (A-C) Anterograde tracing from LHb to RMTg. Diagrams indicate the site of AAV2-GFP injection and the sectioning plane for B-K (coronal view on the right). (A) Analysis of the injection site. Coronal section of the LHb 2 weeks after AAV2-GFP virus injection. (B,C) RMTg region of the AAV2-GFP injected brain on adjacent coronal sections. FoxP1^{+} area is encircled, arrowheads point to GFP-positive fibres. (D-K) Metamphetamine (MetA)-induced FosB expression in the RMTg. (D) TH and FosB IHC on a coronal section of the RMTg. Arrowheads point to FosB expression, arrows to TH^{+} cells negative for FosB. (E) *Gad1* fluorescent ISH and FosB IHC on a section adjacent to that shown in D. Arrowheads point to *Gad1*-expressing FosB^{+} cells. Da and Ea show higher magnification single-channel and merged images of the indicated areas of D and E, respectively. (F-K) FosB and FoxP1 IHC in RMTg of metamphetamine-treated (F-H) and control (I-K) mouse. Arrowheads point to co-expressing cells, arrows to non-co-expressing cells. DA, dopaminergic neurons; IPN, interpeduncular nucleus; LHb, lateral habenula; MHb, medial habenula; RMTg, rostromedial tegmental nucleus; RRF, retrorubral field; VTA, ventral tegmental area. Scale bars: 500 µm (D); 100 µm (A-C,Da-K).

Development (2016) 143, 516-529 doi:10.1242/dev.129957

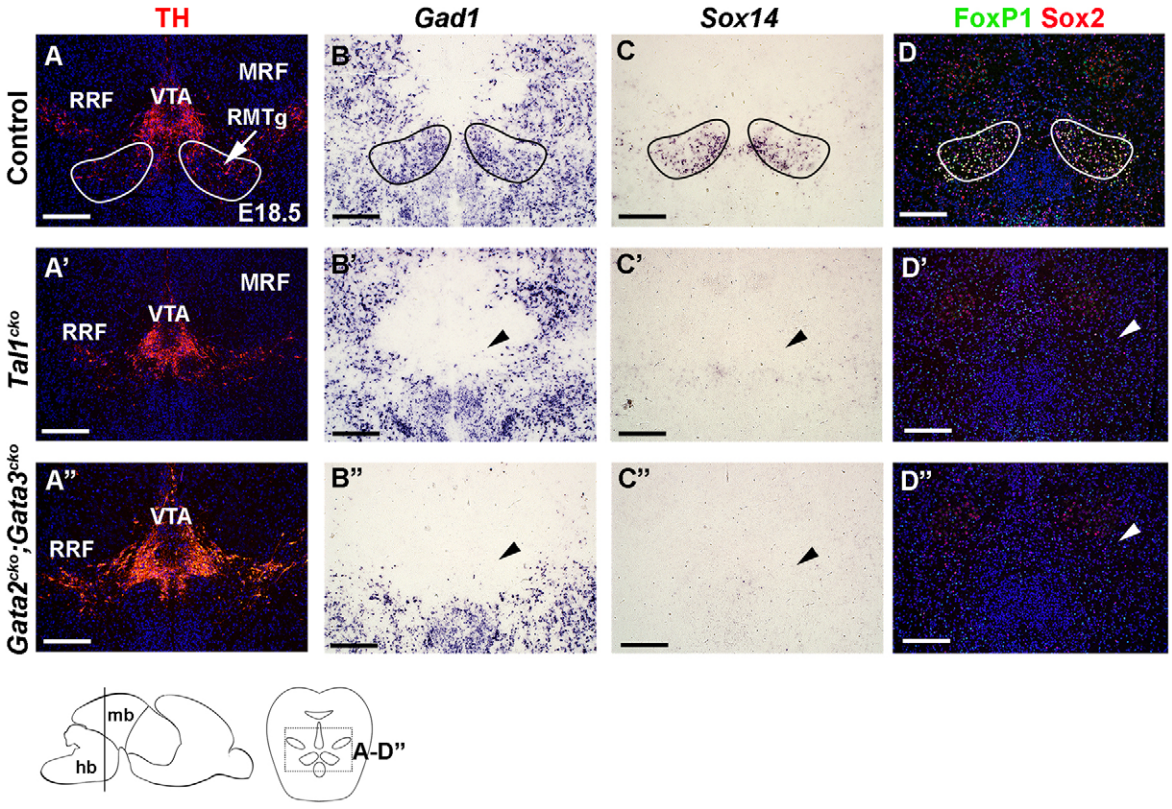

Fig. 7. Loss of RMTg markers in *Tal1*^{cko} and *Gata2*^{cko};*Gata3*^{cko} mutants. (A-D″) IHC (A-A″,D-D″) and ISH (B-B″,C-C″) on adjacent coronal sections of E18.5 control, *Tal1*^{cko} and *Gata2*^{cko};*Gata3*^{cko} embryos. Arrowheads point to altered expression. The level of sectioning is indicated below. hb, hindbrain; mb, midbrain; MRF, midbrain reticular formation; RMTg, rostromedial tegmental nucleus; RRF, retrorubral field; VTA, ventral tegmental area. Scale bars: 200 µm.

sparsely dispersed in the VTA and SNpr (Fig. 8D-Fa). They were labelled in *Gbx2*^{CreERT2};*R26*^{TdTomato} embryos and expressed *Slc17a6*, indicating their origin in r1 and glutamatergic neuronal identity, respectively (Fig. 8G; Fig. S6J-M).

Nkx6-1^{+} cells have been previously described in the rostral part of the avian IPN (Lorente-Canovas et al., 2012). Consistent with this, numerous glutamatergic Nkx6-1^{+}Vsx2^{+} and Nkx6-1^{+} cells born in the r1 were discovered in the IPN (Fig. 8H-K; Fig. S6N-Nb). These cells formed two distinct layers. The top layer, corresponding to IPN rostral (IPNr) and IPN lateral (IPNl) subnuclei, contained mostly Nkx6-1^{+}Vsx2^{+} cells and few Nkx6-1 single-positive cells (Fig. 8H-J). The underlying IPN central (IPNc) subnucleus contained Nkx6-1^{+}Vsx2^{+} cells that co-expressed *Sox14* (Fig. 8O,Oa). Thus, in the r1, *Sox14* transcripts also appear to mark specific glutamatergic neuron subgroups, which might explain why *Sox14* is still expressed in E12.5 *Tal1*^{cko} and *Gata2*^{cko};*Gata3*^{cko} mutants when the other D-GABAergic markers are downregulated. The IPNc contained also r1-derived Pax7^{+}, Zfpm2^{+}, and Pax7^{+}Zfpm2^{+} GABAergic neurons, which in turn lacked Nkx6-1 and *Sox14* expression (Fig. 8L,N,Na,P-Qa). In the adult IPN, Nkx6-1 and Vsx2 were still expressed (Fig. 8M), as were *Pax7*, *Zfpm2* and *Sox14*, although the latter was drastically downregulated (data not shown).

The LDTg contains GABAergic, glutamatergic and cholinergic neurons (Wang and Morales, 2009). At E16.5 and E18.5, we discovered Nkx6-1^{+}, Vsx2^{+}, and Nkx6-1^{+}Vsx2^{+} glutamatergic neurons in an area lateral to the dorsal raphe (DR), corresponding to the LDTg (Fig. 8R-Ua). These neurons formed two groups: a dorsal Nkx6-1^{+} and a ventral Vsx2^{+} population (Fig. 8S,T). A small group of double-positive neurons resided between these two nuclei (Fig. 8Ta). All these neurons were labelled with Gbx2^{CreERT2}, indicating their origin in the r1 (Fig. S6O,Oa). In the adult, we found Vsx2^{+} and Nkx6-1^{+} cells near choline acetyltransferase (ChAT)$^{+}$ cholinergic LDTg neurons (Fig. S6P-Ua). However, Nkx6-1^{+} neurons lacked ChAT but expressed *Slc17a6*, indicating their glutamatergic identity (Fig. S6V,Va).

Thus, in addition to GABAergic neurons, rV2 generates several subtypes of glutamatergic neurons, which contribute to nuclei both in the midbrain and anterior hindbrain. The transcription factors Vsx2 and Nkx6-1 could be used to identify some of these different subpopulations.

A postmitotic switch from GABAergic to glutamatergic identity in the absence of *Tal1* or *Gata2/3*

Because Tal1 and Gata2/3 factors were required for the GABAergic identity in ventral r1, we investigated whether in the same region they also suppressed the glutamatergic identity. Indeed, when we analysed Nkx6-1^{+}, Vsx2^{+}, and Vsx2^{+}Nkx6-1^{+} precursors in E12.5 *Tal1*^{cko} and *Gata2*^{cko};*Gata3*^{cko} embryos, their numbers were significantly increased in both mz1 and mz2 (Fig. 9A-A″,C). At this stage, *Slc17a6* was expressed in the wild-type rV2 domain at a very low level (Fig. 9B). Although the low expression level made quantification impossible, in both mutants it appeared slightly upregulated (Fig. 9B′,B″). *Gata2*^{cko} and *Gata3*^{cko} single mutants showed no apparent changes either in the number of Nkx6-1^{+} and Vsx2^{+} precursors, or in the expression of *Slc17a6* (Fig. S7).

The upregulation of *Nkx6-1* and *Vsx2* expression in the mutant rV2 domain might represent a mere temporary transcriptional misregulation, rather than a true cell fate change. If the GABAergic neurons were truly switching to glutamatergic identity, we would expect to find more glutamatergic neurons in the areas where these

Development (2016) 143, 516-529 doi:10.1242/dev.129957

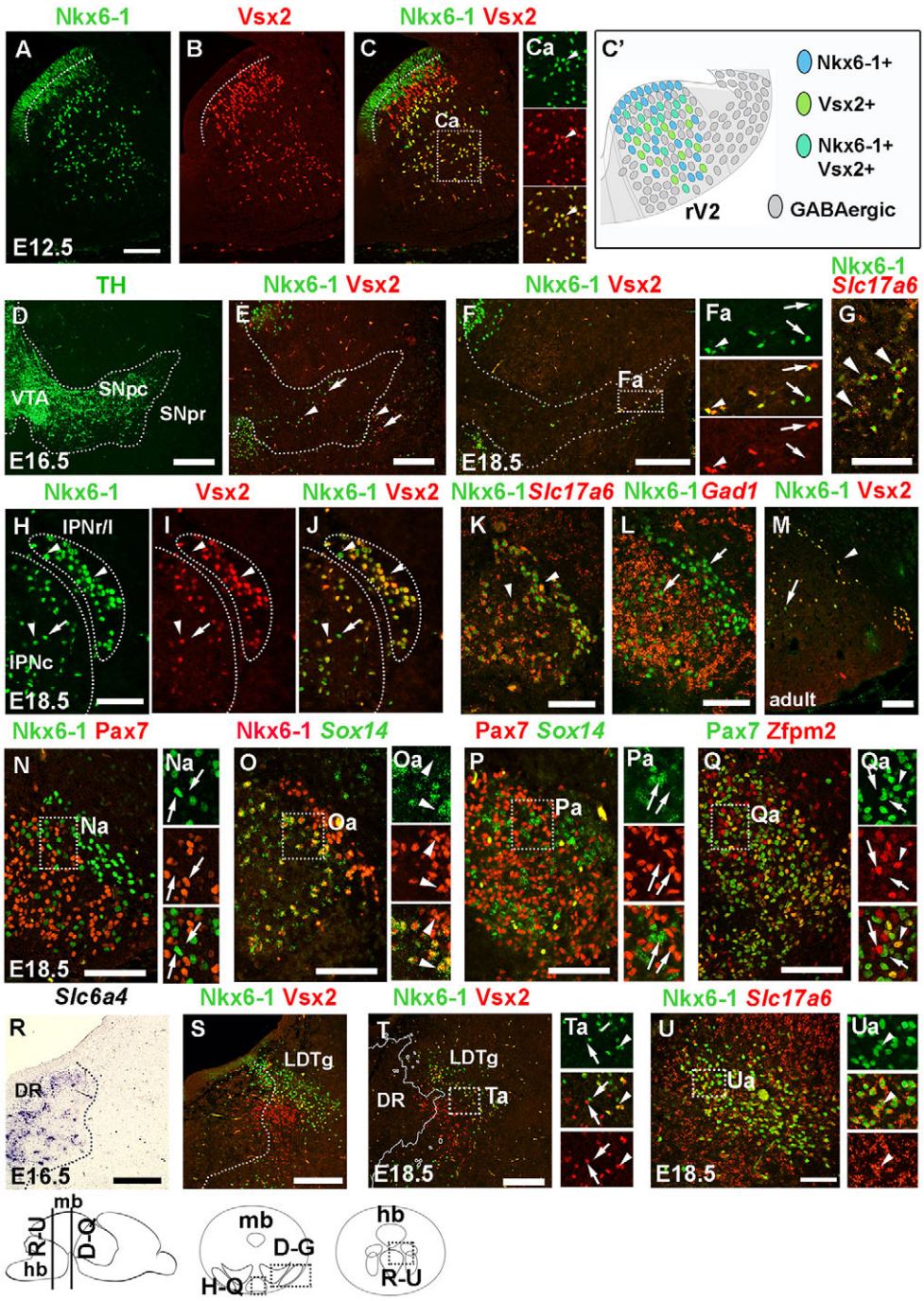

Fig. 8. Nkx6-1^{+} and Vsx2^{+} glutamatergic neurons in the IPN, VTA, SN and LDTg. (A-C) IHC on transverse section of E12.5 r1. Dotted line indicates the ventricular/mantle zone boundary. (C′) Schematic of neuronal subtypes generated in the rV2. (D-F) IHC on E16.5 (D,E) and E18.5 (F) VTA and SN region. TH-staining boundaries on adjacent sections are shown as dotted lines. (G) IHC and fluorescent ISH on E18.5 SNpr. (H-Q) IHC (H-J,M,N,Q) and IHC and fluorescent ISH (K,L,O,P) on IPN sections. (R-U) ISH (R), IHC (S,T) and IHC and fluorescent ISH (U) of the LDTg region in E16.5 (R,S) and E18.5 (T,U) embryos. The dorsal raphe boundaries (dotted lines) are based on *Slc6a4* (R) or 5-HT (not shown) signal on an adjacent section. Ca, Fa, Na, Oa, Pa, Qa, Ta and Ua show higher magnification single-channel and merged images of the indicated areas of C, F, N, O, P, Q, T and U, respectively. Arrowheads indicate co-expressing, and arrows non-co-expressing cells. The level of sectioning is indicated below. DR, dorsal raphe; hb, hindbrain; IPNc, central interpeduncular nucleus; IPNr/l, rostral/lateral interpeduncular nucleus; LDTg, laterodorsal tegmental nucleus; mb, midbrain; SNpc, substantia nigra pars compacta; SNpr, substantia nigra pars reticulata; VTA, ventral tegmental area. Scale bars: 200 µm (A-F,M,R-T); 100 µm (G,H-L,N-Q,U).

neurons normally reside, including the IPN, SN, VTA and LDTg. Indeed, in E18.5 *Tal1^{cko}* and *Gata2^{cko};Gata3^{cko}* mutants IPNr, IPNl, SNpr and LDTg all contained more Nkx6-1^{+}, Vsx2^{+}, and Nkx6-1^{+}Vsx2^{+} neurons (Fig. 10A-A‴,C-D‴). No significant difference was observed in the VTA (Fig. 10B-B‴).

Taken together, the loss of GABAergic precursors in the absence of *Tal1* and *Gata2/3* is paralleled by an increased amount of glutamatergic precursors, which later populate specific glutamatergic nuclei in the midbrain and anterior hindbrain.

DISCUSSION

Recent studies have highlighted local GABAergic and glutamatergic neurons in the control of the DA and 5-HT pathways (Fig. 11B) (Zhou and Lee, 2011; Barrot et al., 2012; Lammel et al., 2014; Morales and Root, 2014). Our current results demonstrate that these diverse GABAergic and glutamatergic neurons originate in a specific region of ventrolateral r1 and reveal a molecular framework controlling their differentiation and heterogeneity.

Tal1, Gata2 and Gata3 as selector transcription factors of GABAergic identity

Terminal selector transcription factors establish subtype identities of differentiating neurons and their expression is activated at the cell-cycle exit (Deneris and Hobert, 2014). Our earlier studies demonstrated that Gata2 and Tal2 act as post-mitotic selectors during development of midbrain and diencephalic GABAergic neurons (Kala et al., 2009; Virolainen et al., 2012; Achim et al.,

Development (2016) 143, 516-529 doi:10.1242/dev.129957

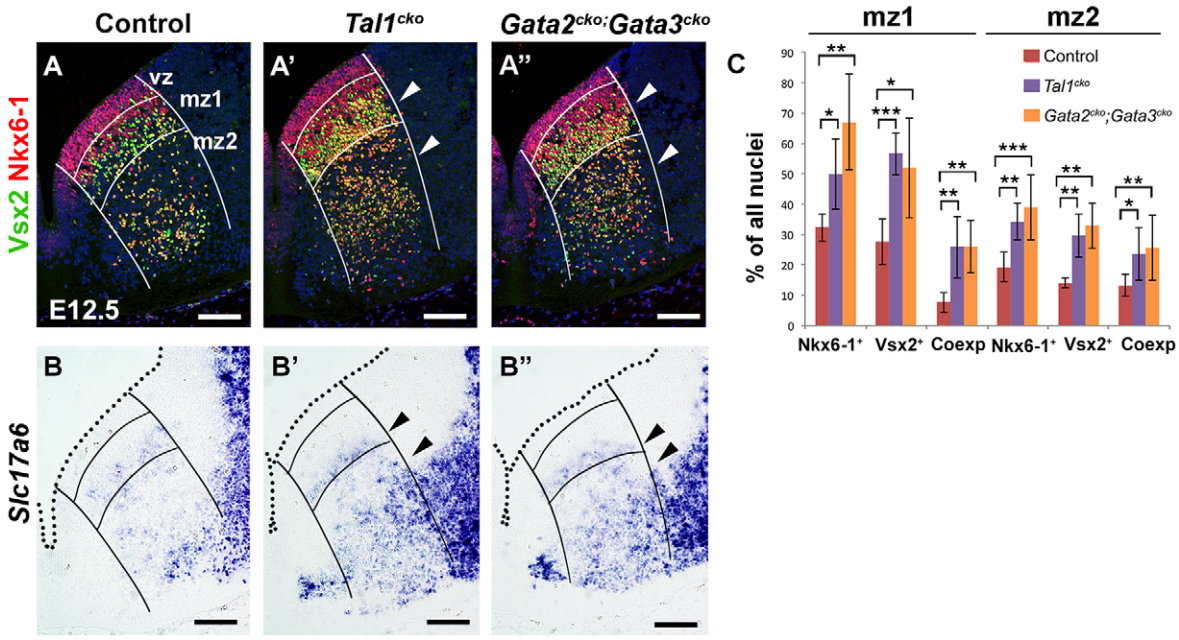

Fig. 9. Increased Nkx6-1^{+} and Vsx2^{+} glutamatergic precursors in *Tal1^{cko}* and *Gata2^{cko};Gata3^{cko}* r1. (A-B″) IHC (A-A″) and ISH (B-B″) on transverse sections of E12.5 control, *Tal1^{cko}* and *Gata2^{cko};Gata3^{cko}* r1. The boundaries of the rV2 domain, vz, mz1 and mz2 are indicated with lines. Arrowheads point to altered expression. Dotted line delineates the ventricular surface. (C) The amount of Nkx6-1^{+}, Vsx2^{+}, and double positive (Coexp) nuclei in the control and mutant mz1 and mz2 (averages with s.d.). *P<0.05, **P<0.01, ***P<0.001. Scale bars: 200 µm.

2013). The midbrain-derived GABAergic precursors contribute to neuronal populations in the superior and inferior colliculi, periaqueductal grey and midbrain reticular formation. Although these midbrain precursors also express Tal1, they do not require it for their differentiation (Achim et al., 2013). Here, we show that the Nkx6-1^{+} rV2 domain in ventral r1 generates a variety of D-GABAergic and glutamatergic cell types expressing subtype-specific transcription factors (Fig. 11A). In contrast to the midbrain GABAergic neurons, Tal1 operates as a selector driving differentiation of D-GABAergic neurons. Without Tal1, postmitotic neuronal precursors in the rV2 mostly fail to activate the gene expression typical for D-GABA subpopulations and assume glutamatergic identities instead. Interestingly, this fate change appears to be complete enough to allow the superfluous glutamatergic precursors to migrate to the glutamatergic subregions of the IPN, SN and LDTg.

During haematopoietic cell differentiation, Tal1 works in a complex with Gata factors (Wadman et al., 1997). Development of D-GABA neurons was not affected by inactivation of *Gata2* or *Gata3* alone. By contrast, GABAergic precursors in rV2 adopted a glutamatergic identity in *Gata2^{cko};Gata3^{cko}* double mutants. Although the phenotypes of *Tal1^{cko}* and *Gata2^{cko};Gata3^{cko}* embryos resembled each other, they also displayed clear differences, the *Gata2^{cko};Gata3^{cko}* mutants showing a more complete loss of D-GABA neurons and their precursors. Thus, these selector factors might have both shared and unique targets. Redundancy between *Gata2* and *Gata3* is not observed in the midbrain or many other GABAergic populations. This could be explained by tissue-specific regulatory mechanisms of *Gata2* and *Gata3* genes. Unlike in the midbrain, where Gata2 is required for *Gata3* and *Tal1* expression (Kala et al., 2009; Achim et al., 2013), in the r1 the three selector genes *Gata2*, *Gata3* and *Tal1* are all activated independently of each other. Indeed, compared with the midbrain, distinct enhancer elements have been shown to drive *Gata2* expression in the r1 (Zhou et al., 2000). Gata2 and Gata3 are also important for the development of serotonergic neurons in the r1 (Craven et al., 2004; Pattyn et al., 2004; Kala et al., 2009). The Gata-regulated neuronal phenotypes, GABAergic and serotonergic, appear to result from the presence or absence of Gata co-factors, especially Tal1.

Development and diversity of GABAergic neurons associated with the midbrain dopaminergic nuclei

Development and molecular heterogeneity of D-GABA neurons are poorly understood. Our results show that the different D-GABA nuclei express unique molecular markers, which correlate with their embryonic origins and anatomical locations (Fig. 11A). In the rV2, these markers are activated in a Gata/Tal-dependent fashion soon after the cell cycle exit. Cells expressing *Zfpm2*, *Sox14*, *En1* and *Gata3* contribute to the neuronal subtypes present in the pSNpr. These subtypes also differ in their requirements for Tal1 and Gata factors, as pSNpr contains a small population of Tal1-independent neurons, which are still Gata2/3 dependent. Thus, differentiation of the D-GABA neuron subtypes might be defined by slight changes in the composition of terminal selector complexes. Compared with the pSNpr, aSNpr neurons appear to be developmentally and molecularly distinct. The aSNpr expresses *Six3*, which is absent in rV2. Moreover, this nucleus remains unlabelled by the *Gbx2^{CreERT2}*-line, supporting its origins outside the hindbrain (Achim et al., 2012). Indeed, recent fate-mapping and gene expression studies suggested that the Six3^{+} aSNpr might originate in the Nkx6-2^{+} domain of the ventrolateral midbrain (Madrigal et al., 2015). Although our earlier results indicated that aSNpr is Gata2 dependent (Achim et al., 2012), its dependency on Gata3 and Tal1 factors remains to be investigated.

Similar to the SNpr, VTA GABAergic neurons also appear to be heterogeneous. GABAergic neurons in the lateral VTA expressing Zfpm2 are of r1 origin and are lost in *Tal1^{cko}* mutants. By contrast, our results indicate that, similar to aSNpr, a small subset of GABAergic cells in the PBP originate outside r1 and express *Six3*,

Development (2016) 143, 516-529 doi:10.1242/dev.129957

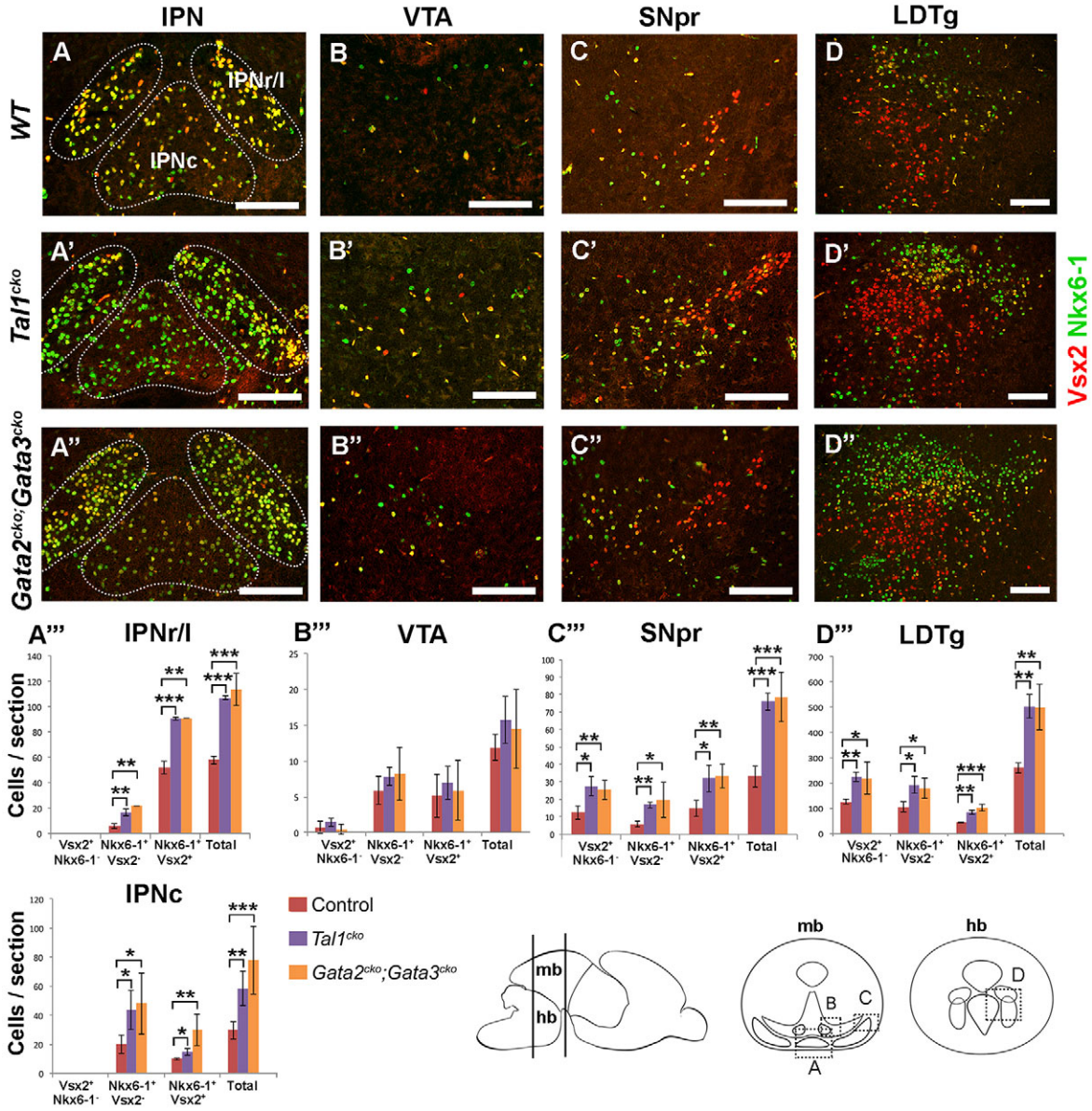

Fig. 10. Increased Nkx6-1^{+} and Vsx2^{+} glutamatergic neurons in *Tal1^{cko}* and *Gata2^{cko};Gata3^{cko}* IPN, SNpr and LDTg. (A-D″) IHC on E18.5 control, *Tal1^{cko}* and *Gata2^{cko};Gata3^{cko}* IPN (A-A″), VTA (B-B″), SNpr (C-C″) and LDTg (D-D″). Subnuclei of IPN are circled in A-A″. (A‴) Quantification of positive cells (average with s.d., A‴-D‴). Sectioning planes and analysed areas are presented at the bottom. hb, hindbrain; IPNc, central interpeduncular nucleus; IPNr/l, rostral/lateral interpeduncular nucleus; LDTg, laterodorsal tegmental nucleus; mb, midbrain; SNpr, substantia nigra pars reticulata; VTA, ventral tegmental area. Scale bars: 200 µm.

suggesting an additional level of heterogeneity between the subregions of the VTA. As up to 40% VTA might consist of GABAergic neurons (Lammel et al., 2014), it is likely that in addition to a few Zfpm2^{+} and Six3^{+} neurons it contains additional, for the time being uncharacterized, GABAergic subtypes. It will be of great interest to study whether the molecularly distinct SNpr and VTA GABAergic neurons are involved in different neuronal circuitries and have specific functions.

Our results suggest that the third D-GABA neuron subgroup, the RMTg, is derived from Sox2^{+}FoxP1^{+}Sox14^{+} precursors in rV2. Furthermore, FoxP1 expression also continues in the adult RMTg, providing a useful marker of this important cell group. Based on its gene expression and dependence on Tal1, the RMTg appears to be a relatively homogeneous cell population compared with the SNpr and VTA.

Development of the excitatory neurons regulating the monoaminergic systems

The glutamatergic neurons in the LDTg and IPN also send inputs to the DA and 5-HT nuclei (Fig. 11B). Interestingly, our results show that these excitatory neurons are developmentally related to inhibitory D-GABAergic neurons. They also originate in the rV2 domain and in the *Tal1^{cko}* and *Gata2^{cko};Gata3^{cko}* mutants, in which GABAergic differentiation fails, the neuronal precursors are redirected towards the glutamatergic LDTg/IPN/SN identity. Thus, in rV2, the Gata/Tal selectors control a balance in development of the inhibitory and excitatory neurons regulating the monoaminergic systems. Our results also reveal molecular heterogeneity among the glutamatergic neurons in the IPN and LDTg. For example, the Nkx6-1^{+}Vsx2^{+} IPN glutamatergic neurons can be divided into *Sox14*-expressing IPNc neurons and *Sox14*-negative IPNr/IPNl

Development (2016) 143, 516-529 doi:10.1242/dev.129957

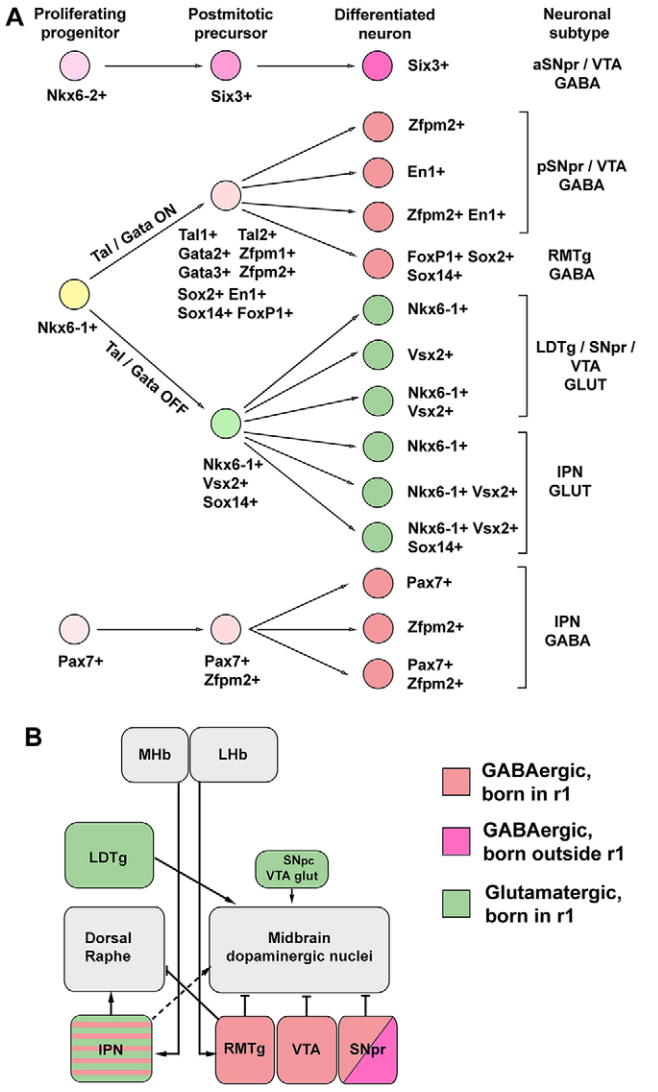

Fig. 11. Glutamatergic and GABAergic subtypes regulating dopaminergic and serotonergic circuits in the mid- and hindbrain. (A) Subtypes of glutamatergic (green) and GABAergic (red) neurons generated in the rV2 domain of r1 from Nkx6-1^{+} progenitors (yellow). Six3^{+} aSNpr GABAergic neurons originate outside r1 (pink). In rV2, Tal1 and Gata2/3 promote GABAergic and suppress glutamatergic identities. Pax7^{+} IPN GABAergic neurons originate from more dorsal r1 progenitors. (B) Involvement of RMTg, LDTg and IPN in inhibitory (GABAergic; red; blunted arrows) and excitatory (glutamatergic; green; arrows) pathways regulating midbrain dopaminergic and dorsal raphe serotonergic neurons. VTA, SNpc and SNpr also contain local inhibitory and excitatory neurons. IPN might regulate dopaminergic neurons via indirect projections (dashed line). aSNpr, anterior substantia nigra pars reticulata; GLUT, glutamatergic; IPN, interpeduncular nucleus; LDTg, laterodorsal tegmental nucleus; LHb, lateral habenula; MHb, medial habenula; pSNpr, posterior substantia nigra pars reticulata; RMTg, rostromedial tegmental nucleus; SNpc, substantia nigra pars compacta; SNpr, substantia nigra pars reticulata; VTA, ventral tegmental area.

neurons. In the LDTg, Nkx6-1 and Vsx2 label primarily two different cell populations.

Recently, glutamatergic tyrosine hydroxylase (TH)-negative neurons have also been demonstrated in the VTA, SNpc/SNpr and RRF (Morales and Root, 2014; Kabanova et al., 2015). We show here that some of them are positive for Nkx6-1 and Vsx2, and their numbers in the SNpr are increased in the *Tal1*^{cko} and *Gata2*^{cko};*Gata3*^{cko} mutants. By contrast, only a few Nkx6-1- or Vsx2-expressing neurons were found in the VTA. Thus, the VTA glutamatergic neurons might constitute a distinct cell group. However, similarly to the D-GABAergic neurons, at least some of the glutamatergic neurons within the DA nuclei appear to be derived from rV2 and differ in their transcription factor profiles from the other midbrain glutamatergic or dopaminergic neurons.

Conclusions

Regulation of the monoaminergic systems is a key to the control of mood, motivation and voluntary movements. Recent studies have described important functions for the brainstem GABAergic and glutamatergic neurons, both in the local regulation of the monoaminergic pathways and as projection neurons affecting forebrain targets. Our study uncovers the developmental origins, molecular mechanisms of differentiation and heterogeneity of these neurons. This will allow more detailed studies of their composition, connectivity and functions.

MATERIALS AND METHODS

Generation and genotyping of mice and embryos

The *En1*^{Cre} (Kimmel et al., 2000), *Gbx2*^{CreERT2} (Chen et al., 2009), *Tal1*^{flox} (Bradley et al., 2006), *Gata2*^{flox} (Haugas et al., 2010), *Gata3*^{flox} (Grote et al., 2008) and *R26*^{TdTtomato} (Madisen et al., 2010) alleles were maintained in an outbred ICR or C57BL/6 background (*R26*^{TdTtomato}) and intercrossed to generate *En1*$^{Cre/+}$;*Tal1*$^{flox/flox}$ (*Tal1*^{cko}), *En1*$^{Cre/+}$;*Gata2*$^{flox/flox}$ (*Gata2*^{cko}), *En1*$^{Cre/+}$;*Gata3*$^{flox/flox}$ (*Gata3*^{cko}), *En1*$^{Cre/+}$;*Gata2*$^{flox/flox}$;*Gata3*$^{flox/flox}$ (*Gata2*^{cko};*Gata3*^{cko}) and *Gbx2*$^{CreERT2/+}$;*R26*$^{TdTtomato/+}$ embryos. Control embryos, littermates of *Tal1*^{cko} and *Gata2*^{cko};*Gata3*^{cko} mutants, were negative for *Cre* and heterozygous or wild type for the flox alleles and displayed a phenotype similar to wild-type (ICR) embryos. E0.5 was defined as noon of the day of the vaginal plug.

Tamoxifen (T5648, Sigma-Aldrich) was dissolved in fresh corn oil (C8267, Sigma-Aldrich) at 20 mg/ml before oral administration at 0.1 mg/g of body weight to pregnant *R26*^{TdTomato} females at noon of E8.5.

The animal experiments were approved by the National Committee of Experimental Animal Research in Finland and carried out according to the National Institutes of Health (NIH) guidelines. AAV work was approved by the National Board for Gene Technology in Finland.

Histology

Embryos were fixed in 4% paraformaldehyde (PFA; Sigma-Aldrich P6148) in PBS. For adult brains, mice were intracardially perfused first with PBS and then with 4% PFA, and postfixed in 4% PFA. All samples were dehydrated and embedded in Histosec polymer wax (Merck Millipore) using a Leica tissue processor ASP300 and sectioned at 5-6 µm.

mRNA ISH and IHC

Non-radioactive mRNA ISH was carried out as described (Wilkinson and Green, 1990), with modifications (Lahti et al., 2012). Fluorescent ISH signal was visualized with anti-DIG-POD (1:1000, Roche) and TSA labelling kits (1:100, FITC or Cy3 dye; PerkinElmer). The DIG-labelled RNA probes were transcribed from plasmids previously described (Jukkola et al., 2006; Kala et al., 2009; Achim et al., 2013). Additional probes were mouse *Sox14* (IMAGp998A2414391Q), *Six3* (IMAGE 5719986) and *cTal1* (a gift from David Rowitch, University of California, San Francisco, CA, USA).

IHC was performed as described (Jukkola et al., 2006) using the primary antibodies listed in Table S1. All secondary antibodies were Alexa Fluor conjugated (1:400, Invitrogen) and nuclei were visualized with DAPI (4′-6′-diamidino-2-phenylindole; Sigma-Aldrich).

Stereotaxic injections

C57BL/6JOlaHsd female mice (16 weeks old) were anaesthetized with isoflurane, attached to the stereotaxic frame (Stoelting, Wood Dale, IL, USA), and small holes were drilled into the skull. Each animal received a unilateral 0.5 µl injection at a speed of 0.5 µl/min using a microinjector (Stoelting, Wood Dale, IL, USA) and microsyringe (NanoFil 33 G, World

Development (2016) 143, 516-529 doi:10.1242/dev.129957

Precision Instruments) of the ssAAV2-eGFP viral vector (8.1×10^{12} vg/ml, UNC vector core, Chapel Hill, NC, USA) to the following coordinates: AP −1.5, DV −2.8, ML −1.2, at a 10° angle. The coordinates were obtained and empirically refined from the mouse brain atlas (Paxinos and Franklin, 2012). Two weeks after the injections, the mice were intracardially perfused and the brains were collected.

Methamphetamine treatment

Male ICR mice (16 weeks old) received two injections of either methamphetamine hydrochloride (Sigma-Aldrich; 10 mg/kg of body weight, s.c., n=4) or corresponding volume of vehicle (0.9% NaCl, s.c., n=2), at 2-h intervals. The mice were housed individually after the first injection. Two hours after the second injection, the mice were intracardially perfused and the brains were collected.

In ovo electroporations

Anterior ventral hindbrain of HH14-16 embryos were electroporated with a plasmid containing *GFP* cDNA under the *Nkx2-2* enhancer (*Nkx2-2-GFP*; a gift from Johan Ericson, Karolinska Institute, Stockholm, Sweden) with or without a vector in which mouse *Tal1* cDNA was placed under the *Nkx2-2* enhancer (*Nkx2-2-mTal1*). Electroporated embryos were incubated at 38°C for 48 h before collection for analysis (n=7 in both groups).

Imaging and statistical analysis

Micrographs were taken using an Olympus BX63 connected to a DP72 camera, and processed with Adobe Photoshop CS6. Brightness, contrast and sharpness were adjusted to recapitulate the original samples as they were seen through the microscope. For each experiment, a minimum of three embryos representing each stage and genotype were analysed. For cell quantification, a minimum of three sections from each area analysed were counted per embryo, except for E12.5 embryos for which the analysis comprised the entire r1. The results were analysed using Student's t-test (*P<0.05, **P<0.01, ***P<0.001).

Acknowledgements

We thank Eija Koivunen, Outi Kostia, Eeva Partanen and Laura Lopez-Blanch for expert technical assistance; and Francesca Morello, Anna Kirjavainen, Esa Korpi and Tapio Heino for discussions and comments.

Competing interests

The authors declare no competing or financial interests.

Author contributions

J.P. directed the project, analysed data and wrote the manuscript together with M.S.; L.L. designed and performed most of the experiments, analysed data, prepared images, and wrote the manuscript; M.H. and L.T. designed and performed experiments, prepared images, and analysed data; S.K. and C.I. performed experiments and analysed data; M.A., M.H.V. and J.A. designed and performed experiments, including stereotaxic injections, and wrote the manuscript.

Funding

This work was supported by the Academy of Finland (J.P., L.L., M.A., J.A., M.H.V.); Sigrid Juselius Foundation (J.P., M.S.); University of Helsinki (M.H.); Center for International Mobility (CIMO; L.T.); Otto A. Malm foundation (L.T.); Integrative Life Sciences doctoral program (L.T.); Ella and Georg Ehrnrooth Foundation (L.L.); and Jane and Aatos Erkko Foundation (J.P.).

Supplementary information

Supplementary information available online at
http://dev.biologists.org/lookup/suppl/doi:10.1242/dev.129957/-/DC1

References

Achim, K., Peltopuro, P., Lahti, L., Li, J., Salminen, M. and Partanen, J. (2012). Distinct developmental origins and regulatory mechanisms for GABAergic neurons associated with dopaminergic nuclei in the ventral mesodiencephalic region. *Development* **139**, 2360-2370.

Achim, K., Peltopuro, P., Lahti, L., Tsai, H.-H., Zachariah, A., Åstrand, M., Salminen, M., Rowitch, D. and Partanen, J. (2013). The role of Tal2 and Tal1 in the differentiation of midbrain GABAergic neuron precursors. *Biol. Open* **2**, 990-997.

Antolin-Fontes, B., Ables, J. L., Gorlich, A. and Ibanez-Tallon, I. (2015). The habenulo-interpeduncular pathway in nicotine aversion and withdrawal. *Neuropharmacology* **96**, 213-222.

Arber, S. (2012). Motor circuits in action: specification, connectivity, and function. *Neuron* **74**, 975-989.

Aroca, P., Lorente-Canovas, B., Mateos, F. R. and Puelles, L. (2006). Locus coeruleus neurons originate in alar rhombomere 1 and migrate into the basal plate: studies in chick and mouse embryos. *J. Comp. Neurol.* **496**, 802-818.

Barrot, M., Sesack, S. R., Georges, F., Pistis, M., Hong, S. and Jhou, T. C. (2012). Braking dopamine systems: a new GABA master structure for mesolimbic and nigrostriatal functions. *J. Neurosci.* **32**, 14094-14101.

Bourdy, R. and Barrot, M. (2012). A new control center for dopaminergic systems: pulling the VTA by the tail. *Trends Neurosci.* **35**, 681-690.

Bradley, C. K., Takano, E. A., Hall, M. A., Gothert, J. R., Harvey, A. R., Begley, C. G. and van Eekelen, J. A. M. (2006). The essential haematopoietic transcription factor Scl is also critical for neuronal development. *Eur. J. Neurosci.* **23**, 1677-1689.

Brown, M. T. C., Tan, K. R., O'Connor, E. C., Nikonenko, I., Muller, D. and Luscher, C. (2012). Ventral tegmental area GABA projections pause accumbal cholinergic interneurons to enhance associative learning. *Nature* **492**, 452-456.

Chen, L., Guo, Q. and Li, J. Y. H. (2009). Transcription factor Gbx2 acts cell-nonautonomously to regulate the formation of lineage-restriction boundaries of the thalamus. *Development* **136**, 1317-1326.

Cohen, J. Y., Haesler, S., Vong, L., Lowell, B. B. and Uchida, N. (2012). Neuron-type-specific signals for reward and punishment in the ventral tegmental area. *Nature* **482**, 85-88.

Craven, S. E., Lim, K.-C., Ye, W., Engel, J. D., de Sauvage, F. and Rosenthal, A. (2004). Gata2 specifies serotonergic neurons downstream of sonic hedgehog. *Development* **131**, 1165-1173.

Deneris, E. S. and Hobert, O. (2014). Maintenance of postmitotic neuronal cell identity. *Nat. Neurosci.* **17**, 899-907.

Fields, H. L., Hjelmstad, G. O., Margolis, E. B. and Nicola, S. M. (2007). Ventral tegmental area neurons in learned appetitive behavior and positive reinforcement. *Annu. Rev. Neurosci.* **30**, 289-316.

Geisler, S., Derst, C., Veh, R. W. and Zahm, D. S. (2007). Glutamatergic afferents of the ventral tegmental area in the rat. *J. Neurosci.* **27**, 5730-5743.

Groenewegen, H. J., Ahlenius, S., Haber, S. N., Kowall, N. W. and Nauta, W. J. H. (1986). Cytoarchitecture, fiber connections, and some histochemical aspects of the interpeduncular nucleus in the rat. *J. Comp. Neurol.* **249**, 65-102.

Grote, D., Boualia, S. K., Souabni, A., Merkel, C., Chi, X., Costantini, F., Carroll, T. and Bouchard, M. (2008). Gata3 acts downstream of beta-catenin signaling to prevent ectopic metanephric kidney induction. *PLoS Genet.* **4**, e1000316.

Haugas, M., Lillevali, K., Hakanen, J. and Salminen, M. (2010). Gata2 is required for the development of inner ear semicircular ducts and the surrounding perilymphatic space. *Dev. Dyn.* **239**, 2452-2469.

Hoffmann, S. A., Hos, D., Kuspert, M., Lang, R. A., Lovell-Badge, R., Wegner, M. and Reiprich, S. (2014). Stem cell factor Sox2 and its close relative Sox3 have differentiation functions in oligodendrocytes. *Development* **141**, 39-50.

Jhou, T. C., Fields, H. L., Baxter, M. G., Saper, C. B. and Holland, P. C. (2009a). The rostromedial tegmental nucleus (RMTg), a GABAergic afferent to midbrain dopamine neurons, encodes aversive stimuli and inhibits motor responses. *Neuron* **61**, 786-800.

Jhou, T. C., Geisler, S., Marinelli, M., Degarmo, B. A. and Zahm, D. S. (2009b). The mesopontine rostromedial tegmental nucleus: a structure targeted by the lateral habenula that projects to the ventral tegmental area of Tsai and substantia nigra compacta. *J. Comp. Neurol.* **513**, 566-596.

Jukkola, T., Lahti, L., Naserke, T., Wurst, W. and Partanen, J. (2006). FGF regulated gene-expression and neuronal differentiation in the developing midbrain-hindbrain region. *Dev. Biol.* **297**, 141-157.

Kabanova, A., Pabst, M., Lorkowski, M., Braganza, O., Boehlen, A., Nikbakht, N., Pothmann, L., Vaswani, A. R., Musgrove, R., Di Monte, D. A. et al. (2015). Function and developmental origin of a mesocortical inhibitory circuit. *Nat. Neurosci.* **18**, 872-882.

Kala, K., Haugas, M., Lillevali, K., Guimera, J., Wurst, W., Salminen, M. and Partanen, J. (2009). Gata2 is a tissue-specific post-mitotic selector gene for midbrain GABAergic neurons. *Development* **136**, 253-262.

Kaufling, J., Veinante, P., Pawlowski, S. A., Freund-Mercier, M.-J. and Barrot, M. (2009). Afferents to the GABAergic tail of the ventral tegmental area in the rat. *J. Comp. Neurol.* **513**, 597-621.

Kimmel, R. A., Turnbull, D. H., Blanquet, V., Wurst, W., Loomis, C. A. and Joyner, A. L. (2000). Two lineage boundaries coordinate vertebrate apical ectodermal ridge formation. *Genes Dev.* **14**, 1377-1389.

Lahti, L., Peltopuro, P., Piepponen, T. P. and Partanen, J. (2012). Cell-autonomous FGF signaling regulates anteroposterior patterning and neuronal differentiation in the mesodiencephalic dopaminergic progenitor domain. *Development* **139**, 894-905.

Lahti, L., Achim, K. and Partanen, J. (2013). Molecular regulation of GABAergic neuron differentiation and diversity in the developing midbrain. *Acta Physiol.* **207**, 616-627.

Lammel, S., Lim, B. K., Ran, C., Huang, K. W., Betley, M. J., Tye, K. M., Deisseroth, K. and Malenka, R. C. (2012). Input-specific control of reward and aversion in the ventral tegmental area. *Nature* **491**, 212-217.

Lammel, S., Lim, B. K. and Malenka, R. C. (2014). Reward and aversion in a heterogeneous midbrain dopamine system. *Neuropharmacology* **76**, 351-359.

Lavezzi, H. N. and Zahm, D. S. (2011). The mesopontine rostromedial tegmental nucleus: an integrative modulator of the reward system. *Basal Ganglia* **1**, 191-200.

Lorente-Canovas, B., Marin, F., Corral-San-Miguel, R., Hidalgo-Sanchez, M., Ferran, J. L., Puelles, L. and Aroca, P. (2012). Multiple origins, migratory paths and molecular profiles of cells populating the avian interpeduncular nucleus. *Dev. Biol.* **361**, 12-26.

Madisen, L., Zwingman, T. A., Sunkin, S. M., Oh, S. W., Zariwala, H. A., Gu, H., Ng, L. L., Palmiter, R. D., Hawrylycz, M. J., Jones, A. R. et al. (2010). A robust and high-throughput Cre reporting and characterization system for the whole mouse brain. *Nat. Neurosci.* **13**, 133-140.

Madrigal, M. P., Moreno-Bravo, J. A., Martinez-Lopez, J. E., Martinez, S. and Puelles, E. (2015). Mesencephalic origin of the rostral Substantia nigra pars reticulata. *Brain Struct. Funct.* 1-12.

Margolis, E. B., Toy, B., Himmels, P., Morales, M. and Fields, H. L. (2012). Identification of rat ventral tegmental area GABAergic neurons. *PLoS ONE* **7**, e42365.

Morales, M. and Root, D. H. (2014). Glutamate neurons within the midbrain dopamine regions. *Neuroscience* **282**, 60-68.

Morello, F. and Partanen, J. (2015). Diversity and development of local inhibitory and excitatory neurons associated with dopaminergic nuclei. *FEBS Lett.* **589**, 3693-3701.

Pattyn, A., Simplicio, N., van Doorninck, J. H., Goridis, C., Guillemot, F. and Brunet, J.-F. (2004). Ascl1/Mash1 is required for the development of central serotonergic neurons. *Nat. Neurosci.* **7**, 589-595.

Paxinos, G. and Franklin, K. (2012). *Paxinos and Franklin's the Mouse Brain in Stereotactic Coordinates*, 4th edn. San Diego: Academic Press.

Perrotti, L. I., Bolanos, C. A., Choi, K.-H., Russo, S. J., Edwards, S., Ulery, P. G., Wallace, D. L., Self, D. W., Nestler, E. J. and Barrot, M. (2005). DeltaFosB accumulates in a GABAergic cell population in the posterior tail of the ventral tegmental area after psychostimulant treatment. *Eur. J. Neurosci.* **21**, 2817-2824.

Proulx, C. D., Hikosaka, O. and Malinow, R. (2014). Reward processing by the lateral habenula in normal and depressive behaviors. *Nat. Neurosci.* **17**, 1146-1152.

Russo, S. J. and Nestler, E. J. (2013). The brain reward circuitry in mood disorders. *Nat. Rev. Neurosci.* **14**, 609-625.

Sego, C., Goncalves, L., Lima, L., Furigo, I. C., Donato, J., Jr. and Metzger, M. (2014). Lateral habenula and the rostromedial tegmental nucleus innervate neurochemically distinct subdivisions of the dorsal raphe nucleus in the rat. *J. Comp. Neurol.* **522**, 1454-1484.

Virolainen, S.-M., Achim, K., Peltopuro, P., Salminen, M. and Partanen, J. (2012). Transcriptional regulatory mechanisms underlying the GABAergic neuron fate in different diencephalic prosomeres. *Development* **139**, 3795-3805.

Wadman, I. A., Osada, H., Grutz, G. G., Agulnick, A. D., Westphal, H., Forster, A. and Rabbitts, T. H. (1997). The LIM-only protein Lmo2 is a bridging molecule assembling an erythroid, DNA-binding complex which includes the TAL1, E47, GATA-1 and Ldb1/NLI proteins. *EMBO J.* **16**, 3145-3157.

Waite, M. R., Skaggs, K., Kaviany, P., Skidmore, J. M., Causeret, F., Martin, J. F. and Martin, D. M. (2012). Distinct populations of GABAergic neurons in mouse rhombomere 1 express but do not require the homeodomain transcription factor PITX2. *Mol. Cell. Neurosci.* **49**, 32-43.

Wang, H.-L. and Morales, M. (2009). Pedunculopontine and laterodorsal tegmental nuclei contain distinct populations of cholinergic, glutamatergic and GABAergic neurons in the rat. *Eur. J. Neurosci.* **29**, 340-358.

Wilkinson, D. G. and Green, J. (1990). In situ hybridization and the three-dimensional construction of serial sections. In *Postimplantation Mammalian Embryos* (ed. A. J. Copp and D. L. Cockroft), pp. 155-171. Oxford: IRL Press.

Yetnikoff, L., Cheng, A. Y., Lavezzi, H. N., Parsley, K. P. and Zahm, D. S. (2015). Sources of input to the rostromedial tegmental nucleus, ventral tegmental area, and lateral habenula compared: a study in rat. *J. Comp. Neurol.* **523**, 2426-2456.

Zhou, F.-M. and Lee, C. R. (2011). Intrinsic and integrative properties of substantia nigra pars reticulata neurons. *Neuroscience* **198**, 69-94.

Zhou, Y., Yamamoto, M. and Engel, J. D. (2000). GATA2 is required for the generation of V2 interneurons. *Development* **127**, 3829-3838.

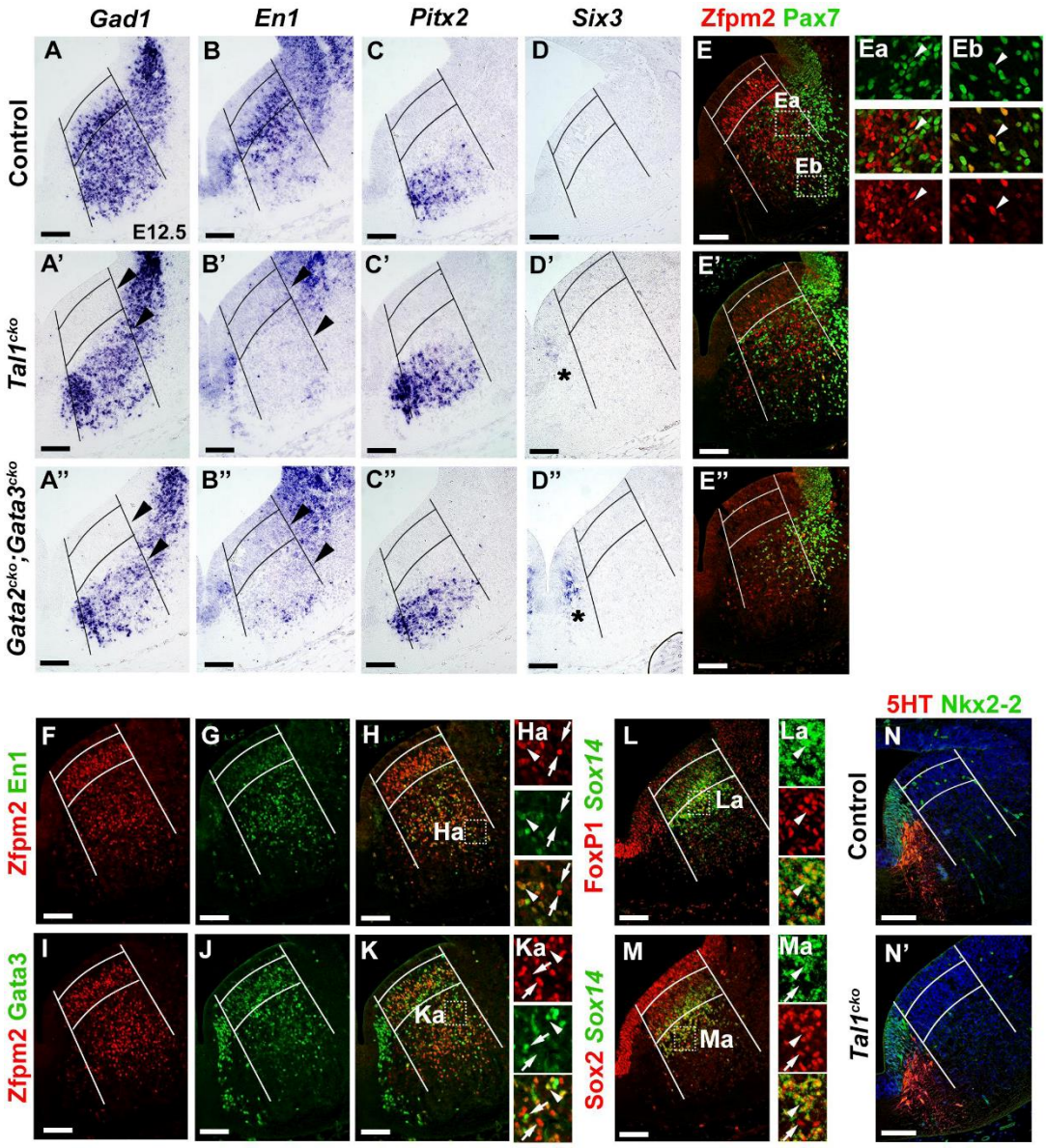

Supplementary Figure S1. Tal1 and Gata2/3 dependent and independent GABAergic neuron subtypes in r1.

(**A-N'**) ISH (A-D''), fluorescent ISH and IHC (L-M, close-ups in La,Ma) and IHC (E-E'',F-K,N,N', with higher magnification images in Ea,Eb,Ha-Ma) of transversal sections of r1. *Gad1* expression is shown here as a reference. The rV2 domain is indicated with lines, with boundaries of ventricular zone (vz), mantle zone 1 (mz1) and mantle zone 2 (mz2) defined similarly as in Figure 1. Black arrowheads (A'-B'') point to altered gene expression. White arrowheads indicate coexpression and white arrows lack of co-expression in (Ea-Ma). An asterisk (*) indicates ectopic Six3 expression, which is detected very weakly in *Tal1*^{cko} (D') and more strongly in *Gata2*^{cko};*Gata3*^{cko} (D'') mutants. This may be indicative of precursor fate transformation in the ventral Nkx2-2^{+} domain of the mutants (M.H., L.T., M.S., J.P., in preparation). Scale bars 200 μm.

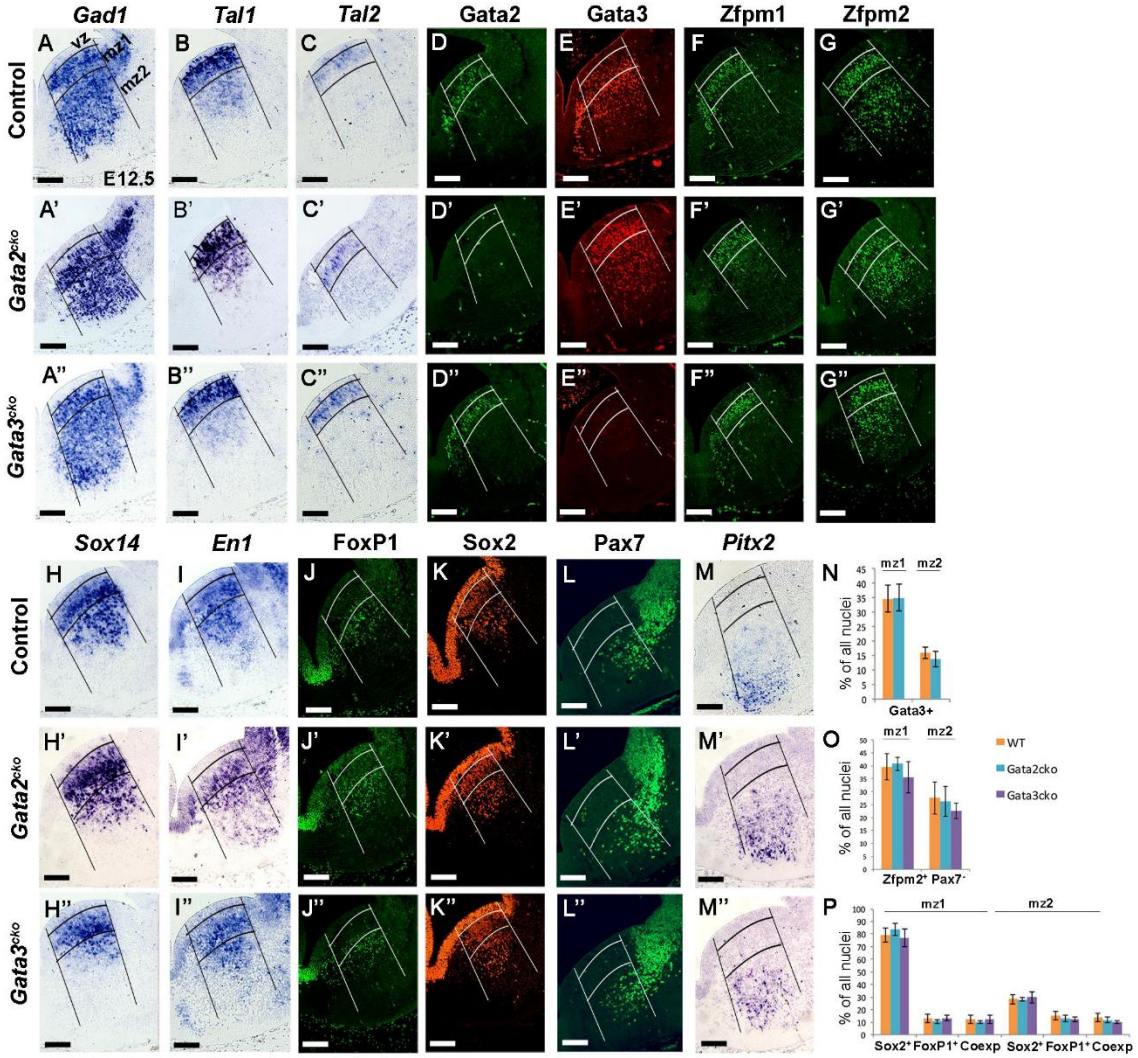

Supplementary Figure S2. GABAergic precursors in *Gata2*^{cko} and *Gata3*^{cko} r1.

(**A-M''**) ISH in (A-C'',H-I'',M-M'') and IHC (D-G'',J-L'') on transversal sections of E12.5 r1 showing no apparent alterations between the control and mutant embryos. The rV2 domain is indicated with lines, and the boundaries of ventricular zone (vz), mantle zone 1 (mz1) and mantle zone 2 (mz2) defined similarly as in Figure 1. (**N-P**) The percentage of Gata3^{+}, Zfpm2^{+}Pax7^{-}, and Sox2^{+}, FoxP1^{+}, Sox2^{+}FoxP1^{+} nuclei represented as averages with s.d. (n=3 in all genotypes). In all comparisons, p>0.05. Scale bars 200 μm.

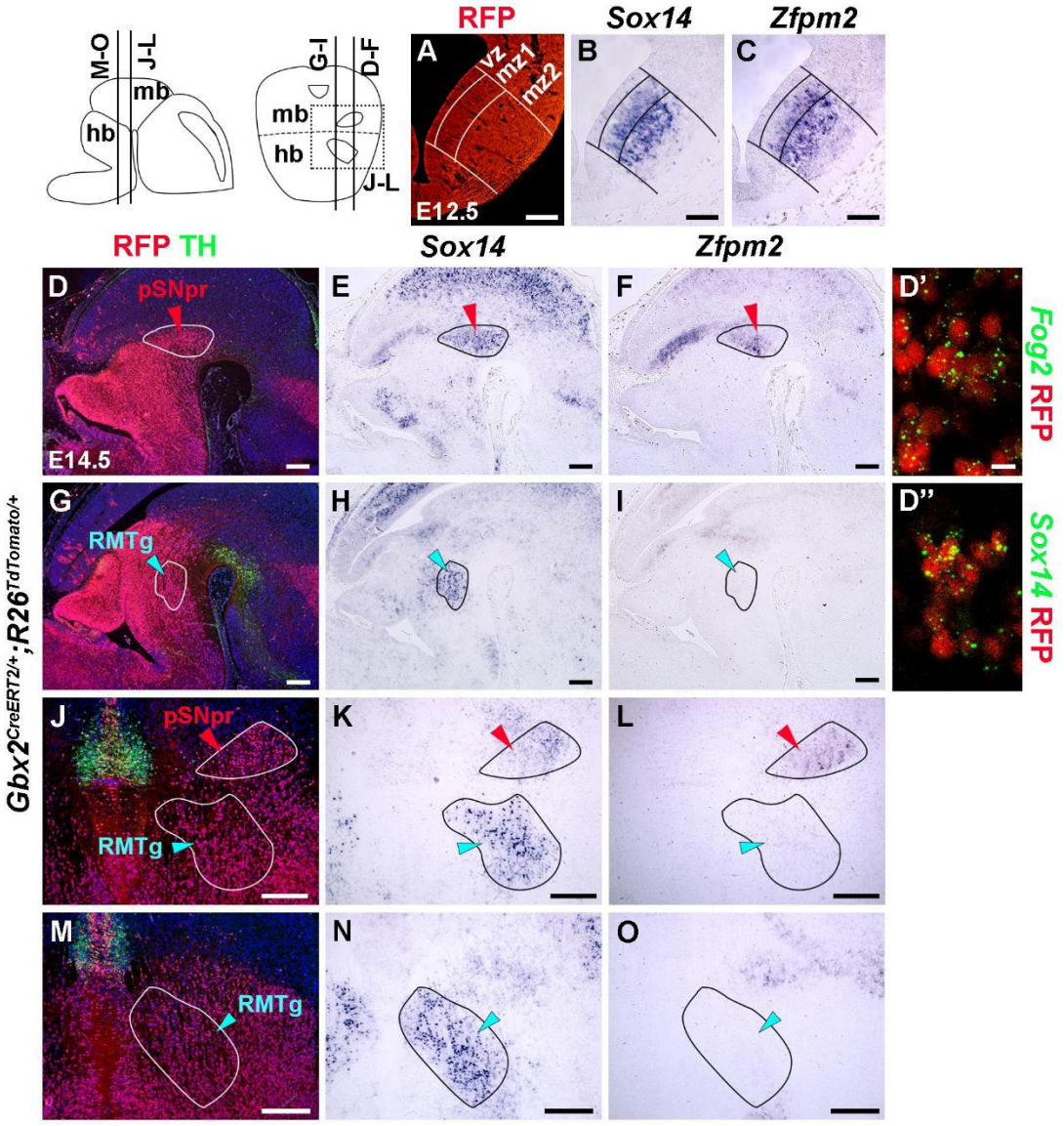

Supplementary Figure S3. Development of pSNpr and RMTg from *Sox14*$^{+}$ and *Zfpm2*$^{+}$ cells in r1.

(**A-C**) IHC (A) and ISH (B-C) on adjacent coronal sections of an E12.5 *Gbx2*^{CreERT2};*R26*^{TdTomato} embryo. The rV2 domain is indicated with lines together with ventricular zone (vz), mantle zone 1 (mz1) and mantle zone 2 (mz2). (**D-O**) IHC (D,G,J,M), ISH (E-F,H-I,K-L,N-O), and combined fluorescent ISH with IHC (D', D'') on sagittal (D-I, D´, D'') and coronal (J-O) sections of E14.5 *Gbx2*^{CreERT2};*R26*^{TdTomato} embryos. (D', D'') close-ups from the SNpr area (indicated in D). RMTg, rostromedial tegmental nucleus; pSNpr, posterior substantia nigra pars reticulata. Scale bars 100 μm in (A-C), 200 μm in (D-O) and 5μm in (D', D'').

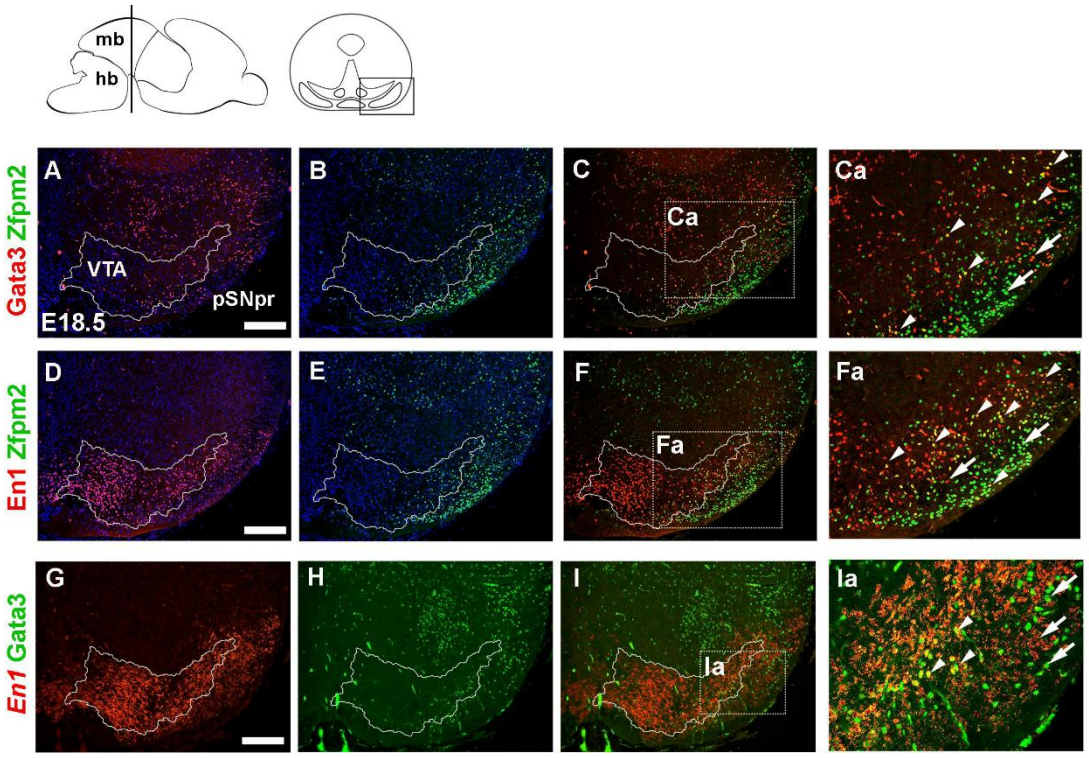

Supplementary Figure S4. GABAergic neuron subtypes in pSNpr.

(**A-Ia**) IHC (A-Fa) and ISH and IHC (G-Ia) on adjacent coronal sections of E18.5 VTA and pSNpr region, with higher magnification images of the boxed areas in (Ca,Fa,Ia). The boundaries of dopaminergic nuclei were based on TH-stainings on a parallel section (not shown). Arrowheads point to coexpressing and arrows to non-coexpressing cells. VTA, ventral tegmental area; pSNpr, posterior substantia nigra pars reticulata. Scale bars 200 μm.

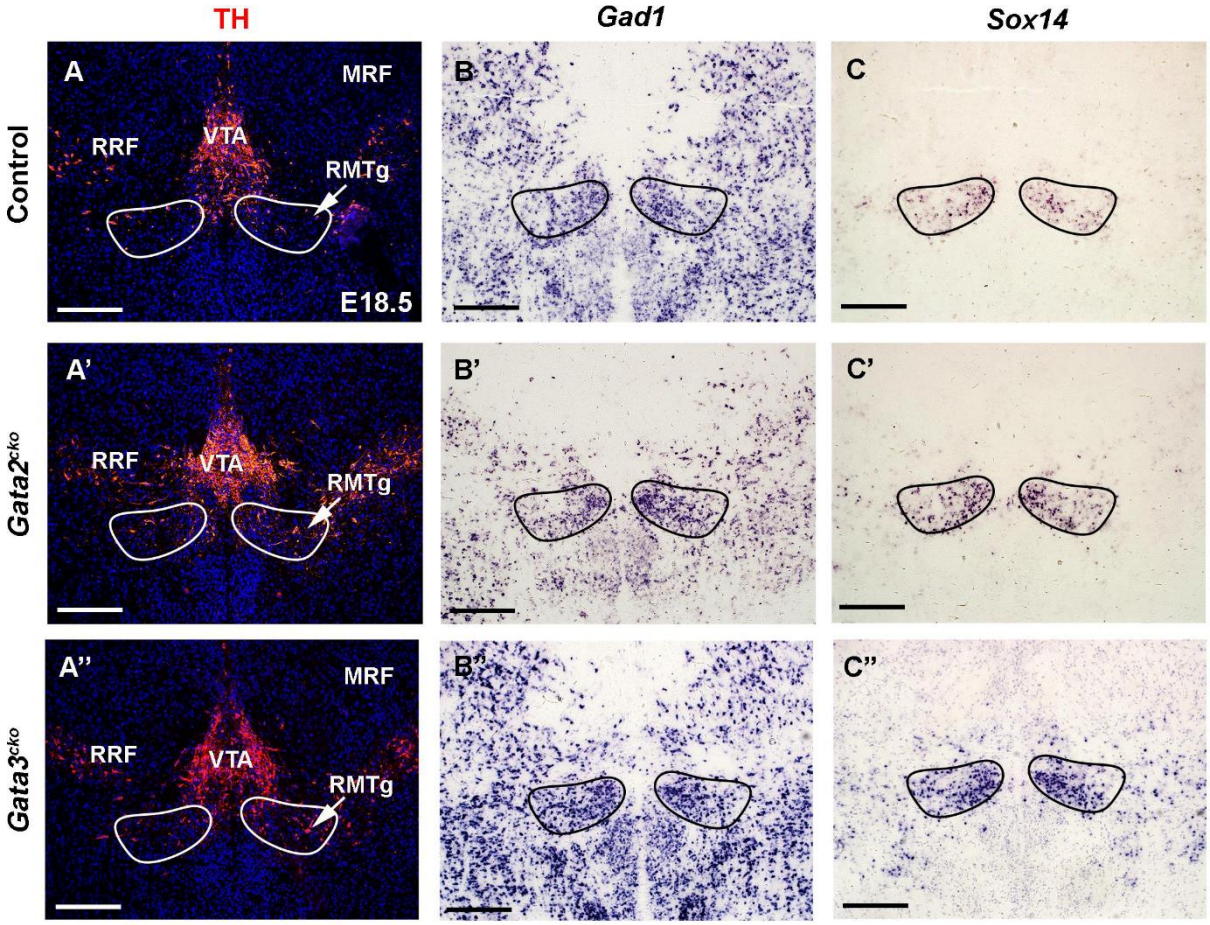

Supplementary Figure S5. RMTg in *Gata2*^{cko} and *Gata3*^{cko} mutants.

(**A-C''**) IHC (A-A'') and ISH (B-C'') on adjacent coronal sections. RMTg is circled based on *Sox14* expression. IPN, interpeduncular nucleus; MRF, midbrain reticular formation; RMTg, rostromedial tegmental nucleus; RRF, retrorubral field; VTA, ventral tegmental area. Scalebars 200 μm.

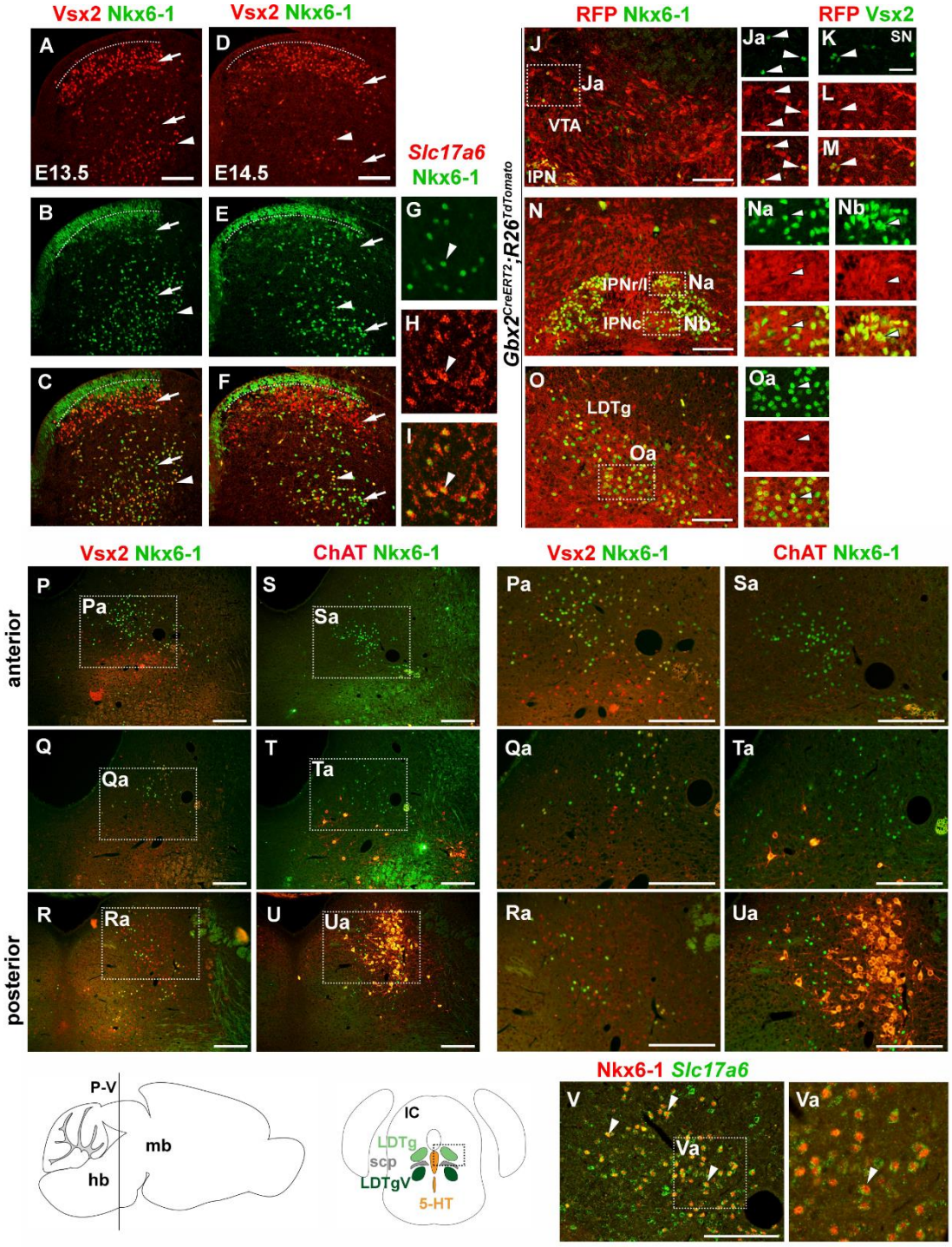

Supplementary Figure S6. Vsx2^{+} and Nkx6-1^{+} glutamatergic neurons in the embryonic and postnatal brain.

(**A-F**) IHC in E13.5 and E14.5 transversal sections of r1, depicting the separation of Vsx2^{+}, Nkx6-1^{+}, and double-positive neuronal populations. (**G-I**) ISH and IHC on E14.5 r1, showing coexpression of *Slc17a6* and Nkx6-1. (**J-O**) IHC on E18.5 *Gbx2*^{CreERT2};*R26*^{TdTomato} embryos from VTA (J,Ja), SN (K-

M), IPN (N-Nb) and LDTg (O-Oa). (**P-Ua**) IHC on adult brain LDTg region, the area indicated in the schematic figure below. Nkx6-1^{+} and Vsx2^{+} are localized near ChAT^{+} cholinergic neurons, but forming their own subnuclei. (**V**) *Slc17a6* ISH and Nkx6-1 IHC on an adjacent section to (P), showing glutamatergic identity of Nkx6-1^{+} neurons. Close-up view (Va). In all images, arrowheads indicate coexpression, and arrows lack of coexpression. 5-HT, serotonergic neurons; hb, hindbrain; IC, inferior colliculus; IPNc, central interpeduncular nucleus; IPNr/l, rostral/lateral interpeduncular nucleus; LDTg, laterodorsal tegmental nucleus; LDTgV, ventral part of laterodorsal tegmental nucleus; mb, midbrain; scp; superior cerebellar peduncle; SN, substantia nigra; VTA, ventral tegmental area. Scalebars 100 μm (A-F,J-O,V), 50 μm (K), 400 μm (P-Ua).

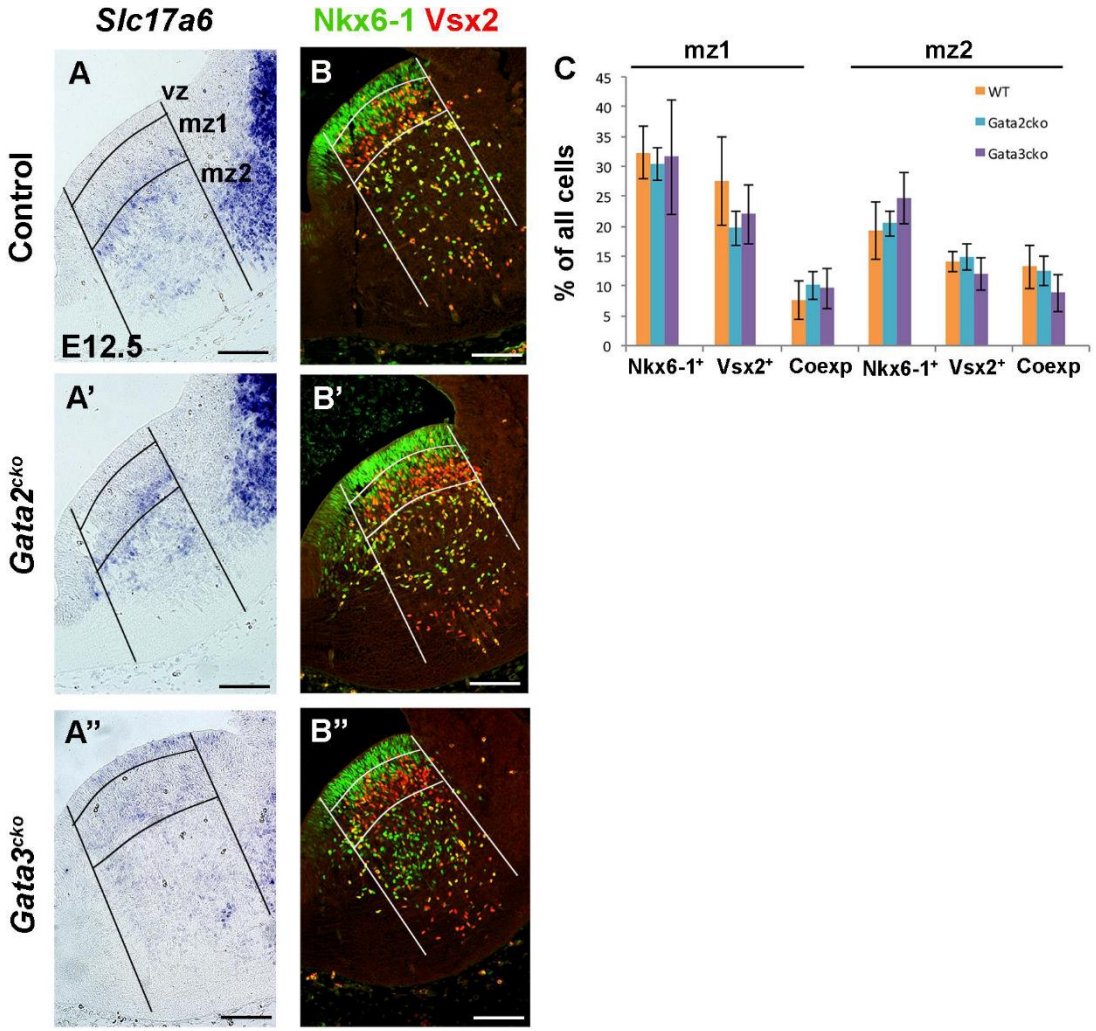

Supplementary Figure S7. Vsx2^{+} and Nkx6-1^{+} glutamatergic neuron precursors in *Gata2^{cko}* and *Gata3^{cko}* r1.

ISH (**A-A''**) and IHC (**B-B''**) on transversal sections of r1. The rV2 domain is indicated with lines, and the boundaries of ventricular zone (vz), mantle zone 1 (mz1) and mantle zone 2 (mz2) defined similarly as in Figure 1. (**C**) The percentages of Nkx6-1^{+}, Vsx2^{+}, and double-positive nuclei in mz1 and mz2, shown as averages with s.d. (n=3 in all genotypes). In all comparisons $p>0.05$. Scale bars 200 μm.

Supplementary Table S1. List of primary antibodies

Antigen	Species raised in	Supplier	Cat. No	Dilution
5-HT	Rabbit	Immunostar	20080	1:500
ChAT	Goat	Merck Millipore	AB144P	1:100
En1	Mouse	Developmental Studies Hybridoma Bank	4G11	1:200
FosB	Rabbit	Santa Cruz Biotechnology	sc-7203	1:400
FosB	Mouse	Abcam	ab11959	1:500
FoxP1	Rabbit	Abcam	ab16645	1:400
Gata2	Rabbit	Santa Cruz Biotechnology	sc-9008	1:200
Gata3	Mouse	Santa Cruz Biotechnology	HG3-3I sc-268	1:200
GFP	Rabbit	Abcam	ab290	1:800
GFP	Mouse	Merck Millipore	MAB3580	1:500
Nkx6-1	Mouse	Developmental Studies Hybridoma Bank	F55A10	1:1000
Olig2	Goat	Neuromics	GT15132	1:200
Pax7	Mouse	Developmental Studies Hybridoma Bank	Pax7	1:400
RFP	Rabbit	Rockland	600-401-379	1:400
Sox2	Rabbit	Merck Millipore	AB5603	1:400
Sox2	Mouse	Abcam	ab79351	1:800
TH	Rabbit	Merck Millipore	AB152	1:500
TH	Mouse	Merck Millipore	MAB318	1:500
Vsx2	Sheep	Abcam	ab16141	1:400
Zfpm1	Goat	Santa Cruz Biotechnology	M-20 sc-9361	1:400
Zfpm2	Rabbit	Santa Cruz Biotechnology	M-247 sc-10755	1:400
Zfpm2	Mouse	Santa Cruz Biotechnology	H-5 sc-398011	1:400